NASA TECHNICAL MEMORANDUM

NASA TM X-1858

NASA TM X-1858

CASE FILE COPY

# THERMIONIC FUEL IRRADIATION EXPERIMENT DESCRIPTION

*by Robert P. Migra, Leonard J. Kaszubinski, and Robert L. Brown*

*Lewis Research Center*
*Cleveland, Ohio*

NATIONAL AERONAUTICS AND SPACE ADMINISTRATION • WASHINGTON, D. C. • AUGUST 1969

NASA TM X-1858

# THERMIONIC FUEL IRRADIATION EXPERIMENT DESCRIPTION

By Robert P. Migra, Leonard J. Kaszubinski, and Robert L. Brown

Lewis Research Center
Cleveland, Ohio

NATIONAL AERONAUTICS AND SPACE ADMINISTRATION

For sale by the Clearinghouse for Federal Scientific and Technical Information
Springfield, Virginia 22151 – CFSTI price $3.00

## ABSTRACT

An instrumented lead-type experiment for the irradiation of encapsulated fuel and insulator specimens at temperatures and fast neutron fluxes that simulate thermionic reactor conditions is described. Fast neutron fluxes are obtained by use of a cadmium and boron carbide shield to remove the thermal neutrons and a portion of the epithermal neutrons. Automatic temperature control of the fuel is obtained by varying a mixture of argon and helium gas in a thin annulus between the primary and secondary containment barriers of the fuel capsule.

# CONTENTS

# THERMIONIC FUEL IRRADIATION EXPERIMENT DESCRIPTION

by Robert P. Migra, Leonard J. Kaszubinski, and Robert L. Brown
Lewis Research Center

## SUMMARY

A lead-type experiment for the irradiation of encapsulated fuel and insulator specimens at temperatures and fast neutron fluxes that simulate thermionic reactor conditions is described. The experiment is irradiated in a 2-inch vertical test hole in the NASA Plum Brook Reactor Facility (PBRF). The important features of the lead facility are as follows: (1) fast neutron irradiation obtained by use of a cadmium plus boron carbide shield to remove thermal neutrons, (2) high-temperature irradiation obtained by use of two noble gas gaps between the fuel specimen and the coolant water, (3) automatic temperature control obtained by regulating the mixture of argon and helium in one of the gas gaps, (4) ability to collect and store all the control gas used for at least two reactor cycles (about 600 hr), and (5) capability of removing the portion of the experiment within the reactor tank through the reactor fuel element transfer chute and transporting it underwater to the hot cells.

## INTRODUCTION

Nuclear reactors that utilize in-core thermionic diodes have been proposed as electrical power sources for space applications. These applications include auxiliary electric power and power for electric propulsion. Considerable efforts are being made in the research and development of fuels for the proposed reactors. These efforts must include evaluation of specimens by reactor irradiations.

An experiment was designed and constructed at the Lewis Research Center to test prototype thermionic fuels at temperatures, heat fluxes, and neutron fluxes that simulate thermionic reactor conditions. Fuel temperature is controlled with a mixture of helium and argon gas (binary gas). Electrical insulator data are also obtained at temperatures that are dependent on the gamma heat generation rate.

This report describes the experiment, as well as important test procedures and hazards considerations. Preliminary testing and major design analyses are presented.

## TEST OBJECTIVES

The objective of the fuel irradiation is to define and extend the useful lifetime of thermionic fuels in the $2600^{\circ}$ to $3140^{\circ}$ F (1700 to 2000 K) temperature range. The physical size of the fuel, the fuel temperature, the heat flux and the neutron flux simulate those of a typical thermionic reactor.

The objective of the insulator test is to obtain resistance and dielectric strength data for candidate insulator materials at approximately $2100^{\circ}$ F (1420 K). The physical size and shape of the insulator specimens simulate the sheath insulator for a typical thermionic reactor fuel element.

## EXPERIMENT CONCEPT

The in-pile tube was designed to irradiate up to three fuel specimens and two insulator specimens at the same time. It is designed to fit into a 2-inch-diameter LD-1 test hole in the NASA Plum Brook Reactor Facility. A cutaway drawing of the reactor tank is shown in figure 1. Figure 2 is a plan view of the reactor core showing the location of test hole LD-1. The location of the major components of the experiment in the reactor facility is shown in figure 3.

The temperature of each of the three fuel specimens is controlled independently. Temperature control is accomplished by varying the mixture of two gases in a gas gap in the heat-transfer path of the fuel specimen. Helium and argon were chosen for the gases because they are inert and because there is a seven to one ratio of the heat conductivities of the two. The volume of the gas lines between the mixing station and the in-pile capsules is small to ensure rapid control response. Exhaust gas storage for two normal reactor cycles is provided because of argon activation.

The insulator test specimens have no temperature control. Heat conducting pins are sized to limit the specimen temperature.

A fast neutron flux is obtained by placing a cadmium (Cd) plus boron carbide ($B_4C$) shield around the in-pile portion to screen out the thermal neutrons. The boron is enriched in the boron-10 ($B^{10}$) isotope.

For safety reasons, the experiment was designed so that any credible accident may physically damage the experiment but will not be dangerous to reactor personnel. The exhaust gas tubing may contain radioactive argon, or fission gases, in the event of a failure. For this reason, it is necessary to maintain the integrity of the binary gas containment at all times. Therefore, two barriers are utilized between the binary gas and the reactor containment atmosphere, or the reactor water cooling system. The only exceptions are the gas holdup tanks which are designed with a large safety factor and are

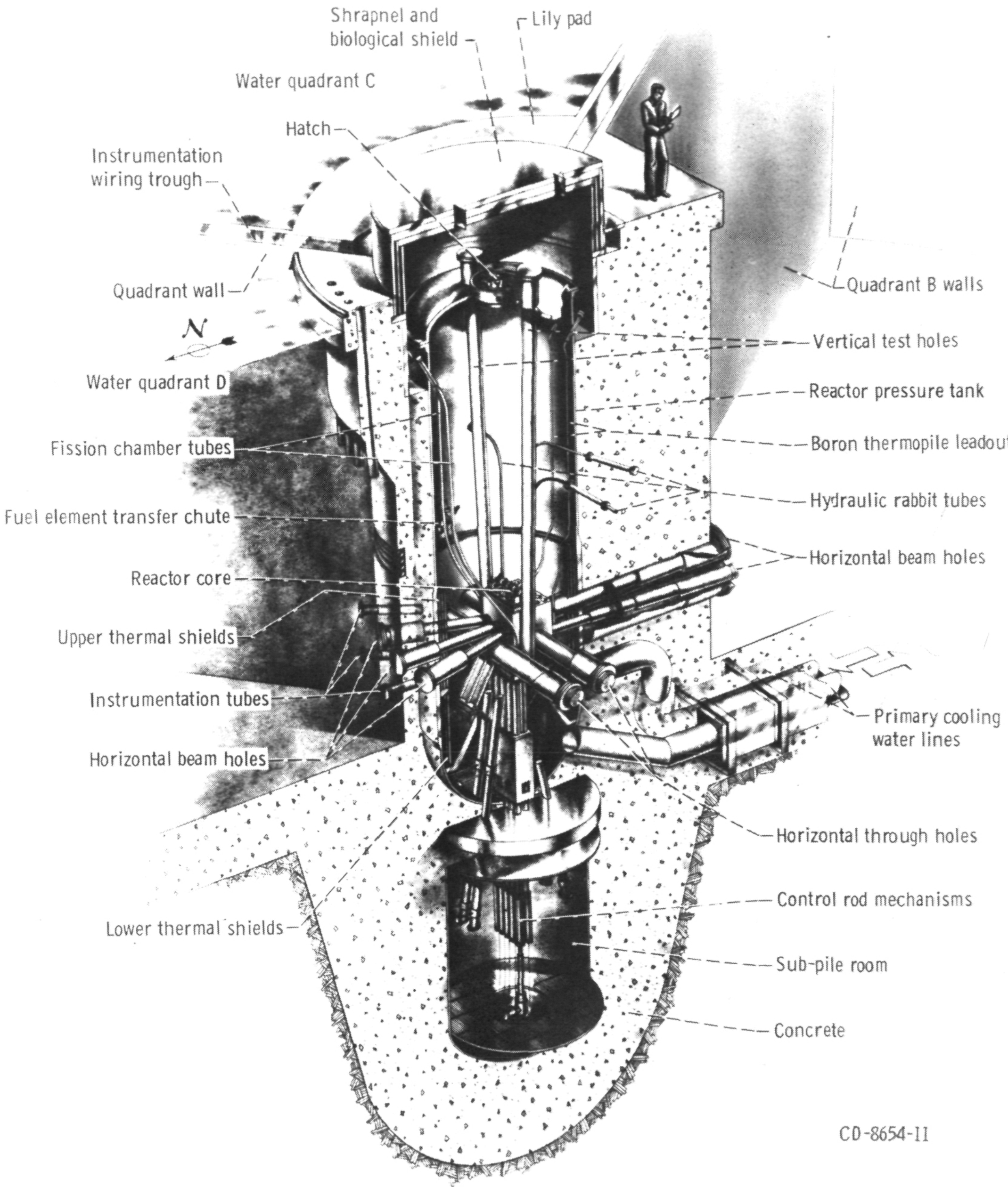


Figure 1. - Cutaway perspective drawing of the Plum Brook Reactor Facility reactor tank assembly.

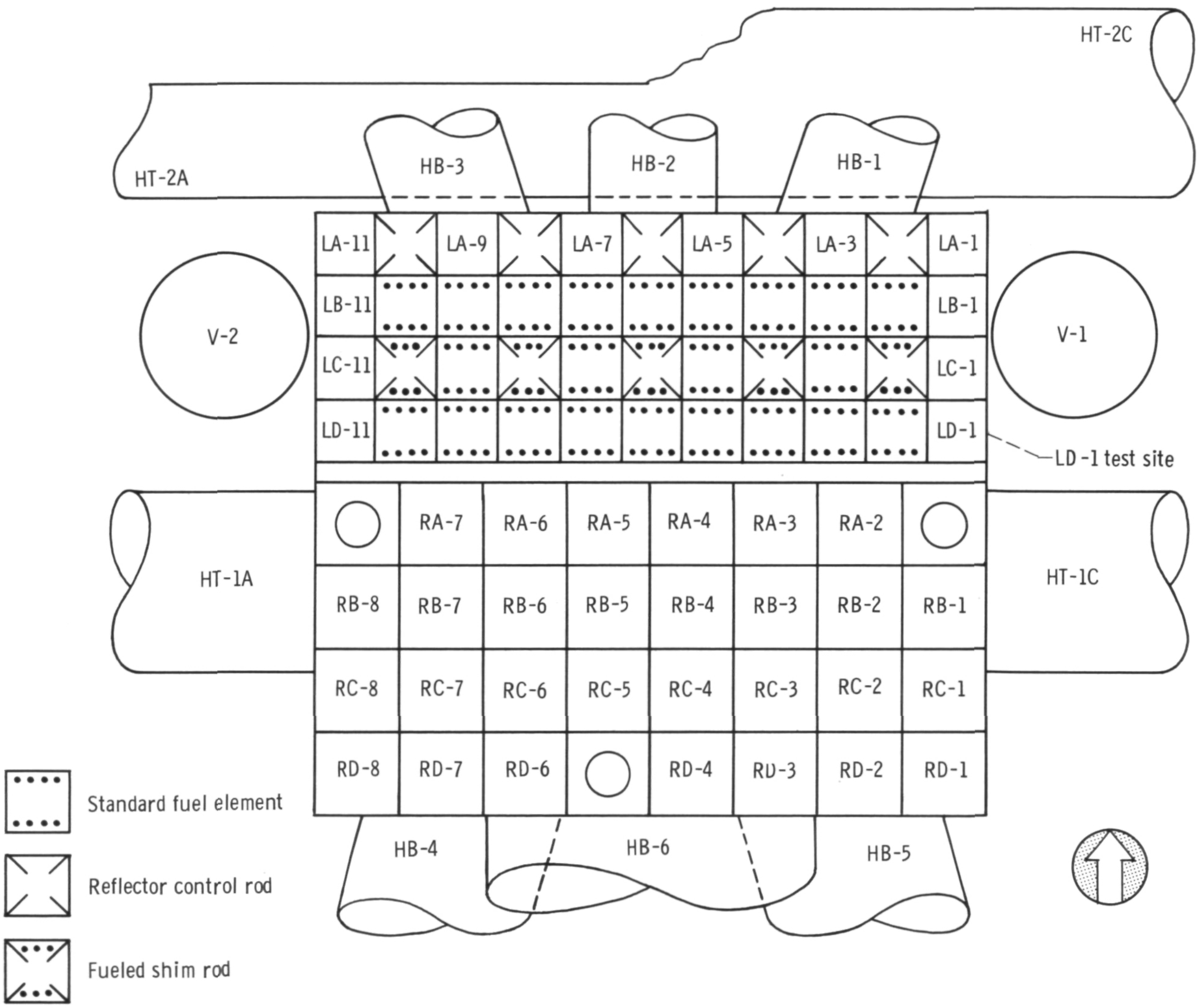


Figure 2. - Plan view of Plum Brook Reactor core and experiment test holes.

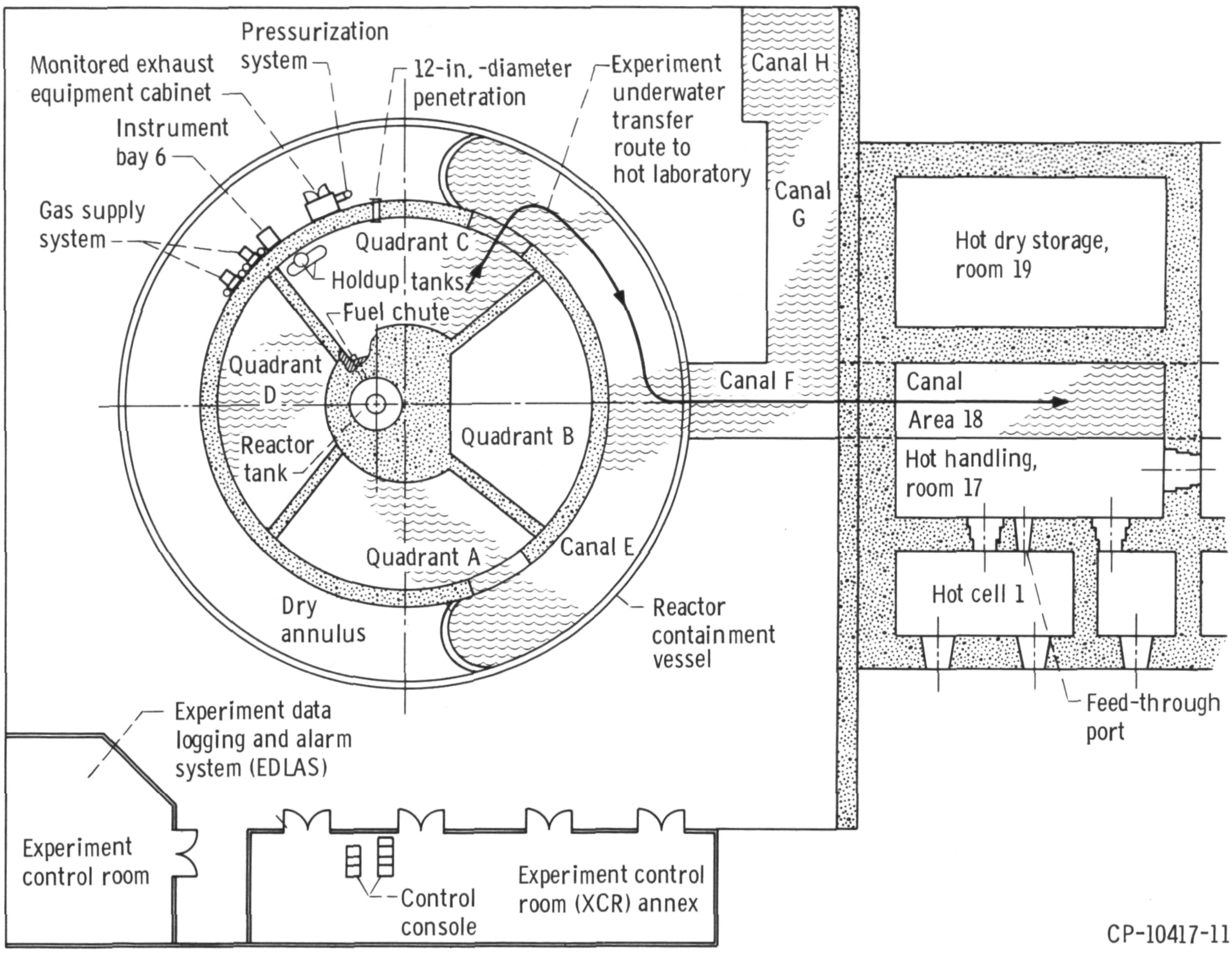


Figure 3. - Plum Brook Reactor Facility reactor building layout.

shielded by 25 feet (7.6 m) of water or 2 feet (0.61 m) of concrete. All lines that may contain radioactive gases are shielded by lead, water, or are located to prevent personnel from approaching too closely while the reactor is operating.

## DESCRIPTION OF EXPERIMENT

The description of the experiment is divided into two parts, namely, the mechanical equipment and the control and instrumentation.

### Mechanical Equipment

The mechanical equipment includes the in-tank assembly (the portion of the experiment within the reactor pressure vessel), the binary gas equipment, and the containment pressurization equipment.

In-tank assembly. - Figure 4 is an overall view of the in-tank assembly. The

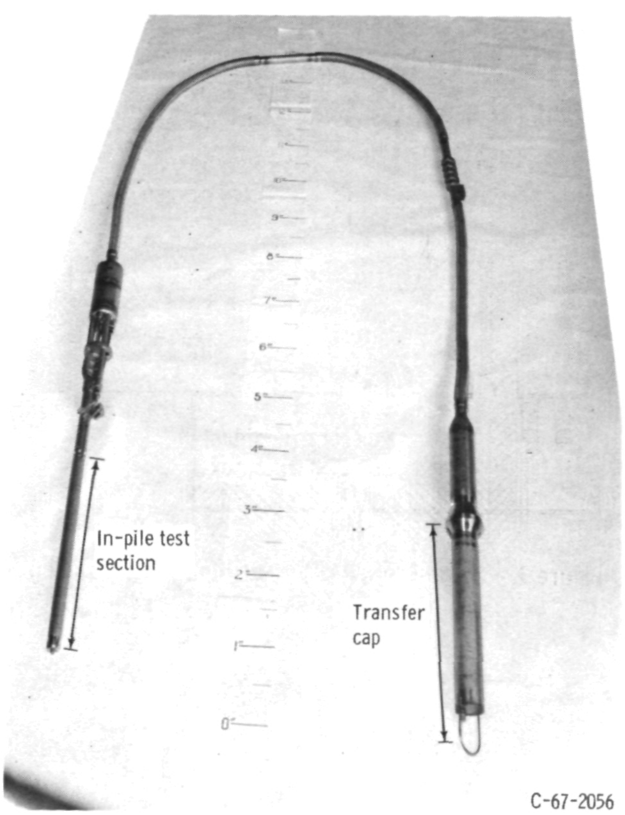


Figure 4. - In-tank assembly showing portion of experiment inside reactor vessel.

upper end is shown sealed with a transfer cap which is provided so that the assembly can be removed underwater through the reactor fuel transfer chute. The transfer cap is removed to install the assembly in the reactor tank. The end of the flexible hose is attached to the junction box which is mounted on a 6-inch (15.2-cm) penetration on the reactor tank. The instrumentation leads and gas lines penetrate into the junction box.

The end of the rigid section contains a maximum of three fuel test capsules and two insulator test capsules. A thermal neutron shield surrounds the test capsules.

A typical fuel capsule (fig. 5) consists of a fuel specimen instrumented with four refractory metal thermocouples. The specimen is surrounded by a primary contain-

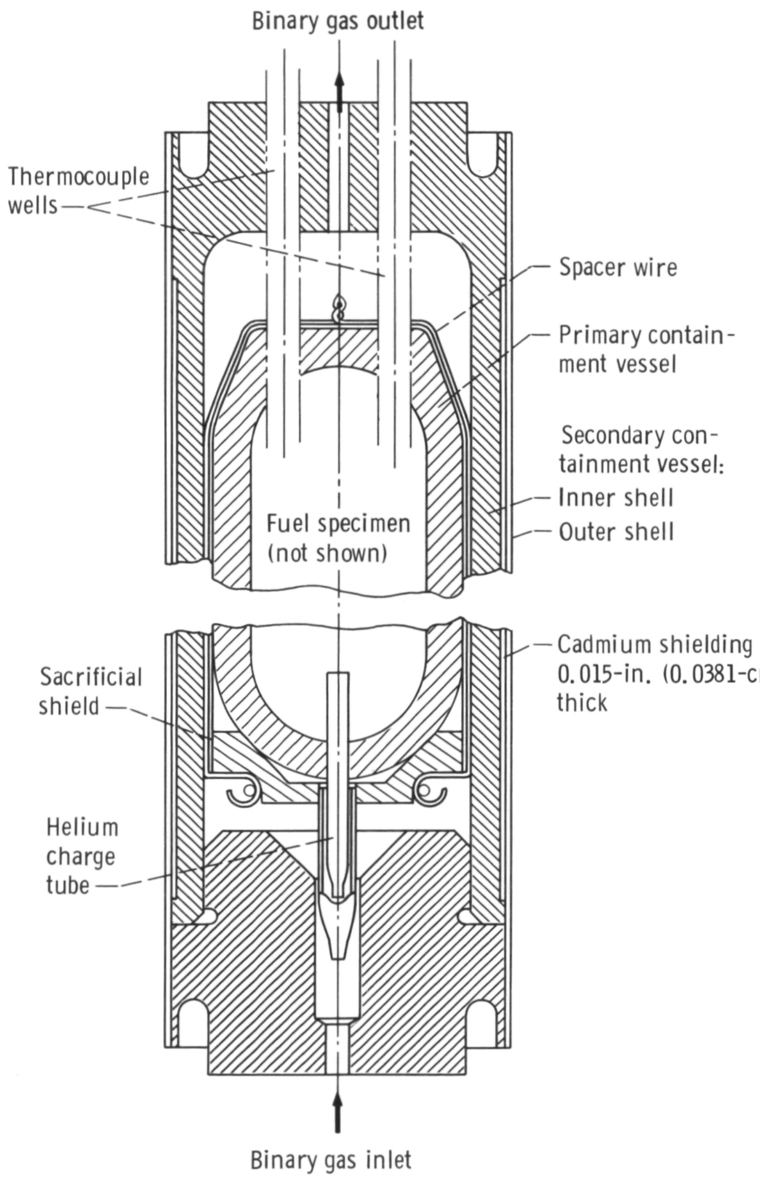


Figure 5. - Fuel capsule structure.

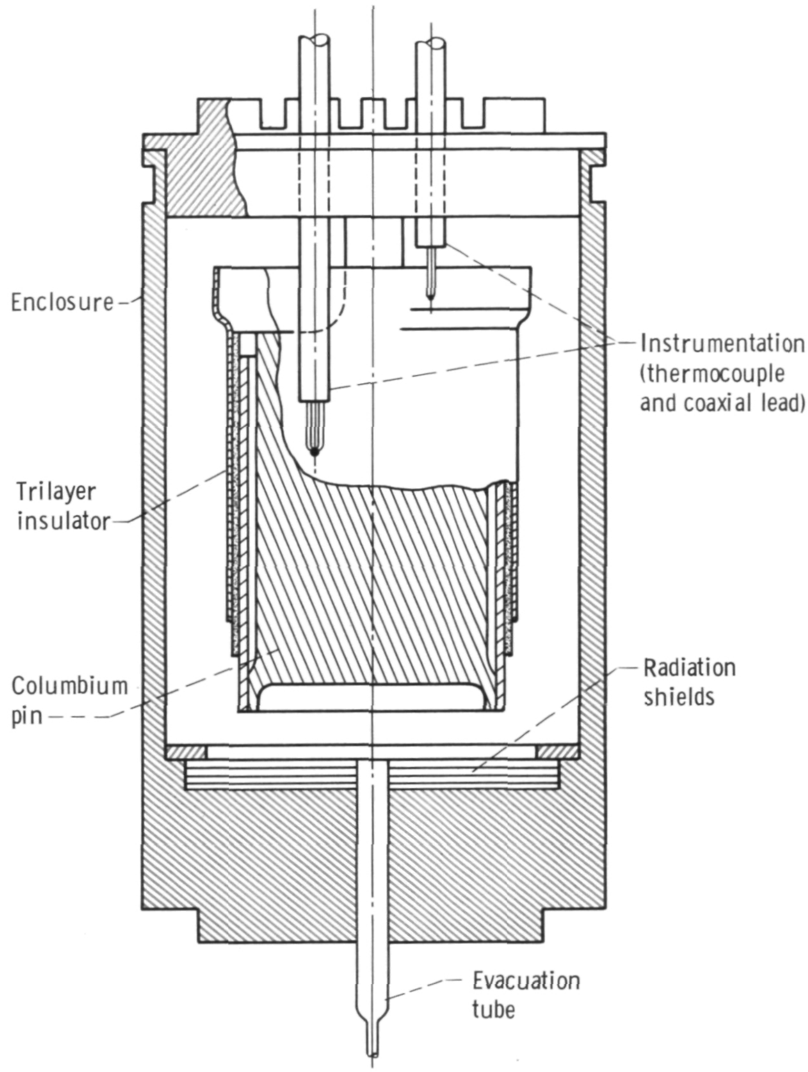


Figure 6. - Insulator test capsule.

ment vessel and a secondary containment vessel. The control gas passes through a 0.01-inch (0.025-cm) annulus between the containment vessels.

A typical insulator test specimen (fig. 6) is enclosed in a stainless-steel capsule. The insulator is instrumented with one Chromel-Alumel thermocouple and a single conductor-shielded lead for resistivity measurements.

Binary gas equipment. - A simplified flow diagram that shows only the main components of the binary gas equipment is given in figure 7. The binary gas equipment is divided into three groups: gas supply, gas-mixing station, and gas exhaust.

Gas supply: The major gas supply components are standard bottles of high-pressure gas, gas manifolds, purifiers, and filters for helium and argon. The manifolds

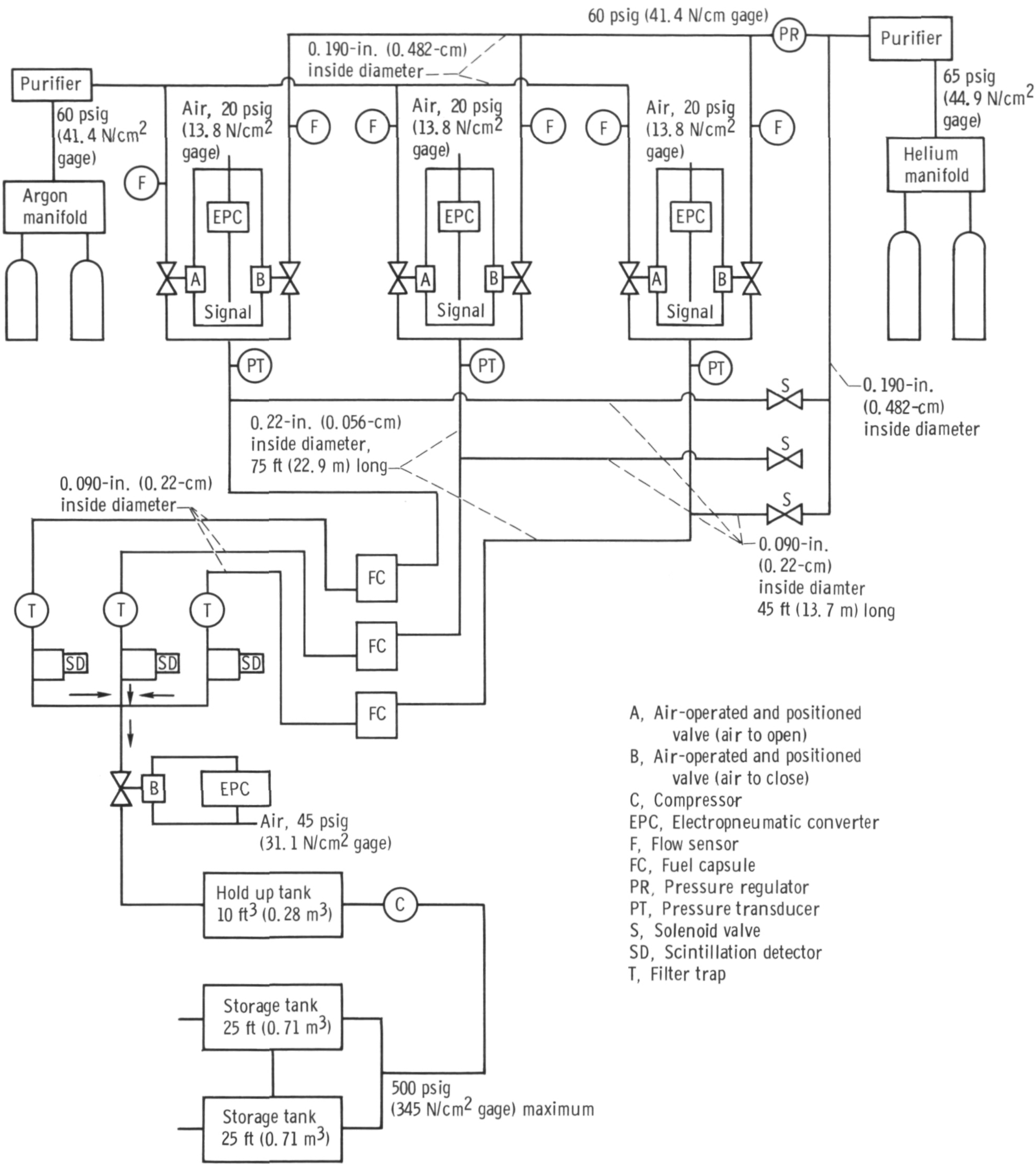


Figure 7. - Binary gas simplified flow diagram.

automatically switch from an empty bottle to a full bottle and regulate the delivery pressure. The purifiers are capable of reducing the oxygen, nitrogen, and water impurities in the gas to below 1 ppm. The filters remove particles greater than 0.08 micrometer from the gas stream.

The helium manifold supplies gas at a higher pressure than the argon manifold. This higher pressure helium supply is used as a helium flush, which is described in the next section. The helium supply for the binary gas is reduced to the argon supply pressure by an additional pressure regulator.

Gas-mixing station: The gas-mixing station is part of the fuel temperature control described later in this report. An overall view is shown in figure 8, and it is shown schematically as part of the flow diagram in figure 7.

The mixing station consists of three identical sections which deliver a separate helium-argon mixture to each of the three fuel capsules. The major components of each section are two flow sensors (one each for helium and argon), a proportioning mechanism, a pressure transducer, and a bypass for helium flushing.

The outputs from the flow sensors are recorded by strip-chart recorders in the

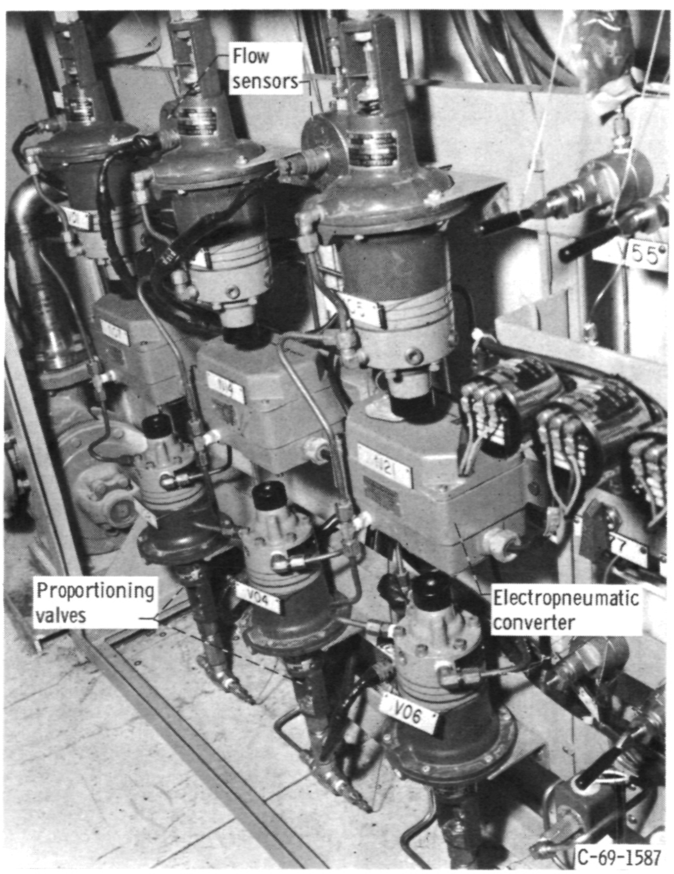


Figure 8. - Gas-mixing station.

control console of the experiment and by the Experiment Data Logging and Alarm System (EDLAS).

Each proportioning mechanism consists of two pneumatically (compressed air) positioned and operated valves (one each for helium and argon) and one electropneumatic converter. The valves are proportional over their ranges. The argon valves are normally closed (i.e., air pressure to open) valves, and the helium valves are normally open (i.e., air pressure to close) valves.

Both of the pneumatic valves in a proportioning mechanism are positioned by the same pneumatic signal from an electropneumatic converter. This pneumatic signal is proportional to an electric error signal that is based on the fuel specimen temperature. An overtemperature in the fuel results in a decreased pressure from the electropneumatic converter, which increases the helium flow and decreases the argon flow. An undertemperature in the fuel increases the signal pressure from the electropneumatic converter, decreasing the helium flow and increasing the argon flow.

The helium flush bypass is provided to ensure rapid and complete helium flooding of the binary gas gap of each capsule if an excessive overtemperature should occur. The helium flooding is accomplished by using a higher pressure, rapidly actuated helium supply that bypasses the proportioning valves and approximately one-half of the small diameter inlet piping. Solenoid valves are used to contain the emergency helium. The valves are opened when the setting of a limit switch on a fuel temperature recorder is exceeded.

The pressures of the binary gas in each section of the gas-mixing station are measured by transducers and are read by meters mounted in the experiment control console. The meters will actuate an alarm if the pressure drops below the alarm setpoint. The setpoint can be set between zero and 75 psig (51.7 $N/cm^2$ gage).

Gas exhaust: The gases in the gas-exhaust equipment may be radioactive. In normal operation of the experiment, argon-41 ($A^{41}$) is present. The maximum total activity of $A^{41}$ in the gas-exhaust system while the test reactor is at full power is 35 millicuries ($1.3\times10^9$ dis/sec). In the event of a failure in the first containment of a fuel capsule, a maximum of 93 curies ($3.4\times10^{12}$ dis/sec) of fission gases may be released to the exhaust equipment. The presence of radioactive gases is accommodated by designing the exhaust equipment to handle and store the total gas flow through the three fuel capsules for two reactor fuel cycles (about 600 hr). The exhaust equipment includes filter traps, scintillation detectors, a compressor, three storage tanks, and miscellaneous equipment (valves, pressure-measuring instrumentation, etc.). The exhaust equipment is shown diagrammatically as a part of figure 7.

The filter traps are provided to remove condensables, such as iodine-131 ($I^{131}$), that might deposit in undesirable places in the system. They consist of a filter section that will remove particles greater than 0.08 micrometer and an "activated" charcoal section that will remove undesirable gases.

Lines from the filter traps pass through water-filled quadrant C and enter the monitored exhaust equipment cabinet (fig. 3). This enclosure was constructed with a minimum of leaks to the surrounding atmosphere. Its purpose is to serve as a "secondary containment" for all components that may contain radioactive gases. Except for the holdup tank, two storage tanks, and the filter traps, all components that may contain radioactive gases are installed in this enclosure. An air pump circulates the air from the enclosure through a remote area monitoring system (RAMS) radiation monitor and back into the enclosure. Just inside of the enclosure, the return lines are monitored for radioactivity using a scintillation counter on each line. After the scintillation counters, the three return lines are manifolded together into a single line. The total return flow passes through a pneumatically operated and positioned valve. This valve is positioned manually from the experiment control console in the experiment control room (XCR) annex.

Next, the binary gas flows into the holdup tank. This tank is provided to allow temporary collection of the binary gas, and thus allows intermittent operation of the compressor. The tank also serves to dilute any radioactive gases that may be released from the capsules.

The compressor is used to move the binary gas from the holdup tank into the storage tanks. It is located in the monitored exhaust equipment container and has a flow capacity of 0.1 standard cubic foot per minute (44 standard $cm^3/sec$) against a head of 500 psig (345 $N/cm^2$ gage). The flow capacity of the compressor is greater with lower head pressures, so that at the normal flow rate of 0.04 standard cubic foot per minute (20 standard $cm^3/sec$), the compressor operates an average of 15 minutes each hour.

The storage tanks are located on the bottom of quadrant C under 25 feet (7.6 m) of water. The tanks are operated independently. At 500 psig (345 $N/cm^2$ gage), each tank is capable of storing 875 standard cubic feet (24.8 standard $m^3$) of gas, which is 105 percent of the amount of binary gas used during a normal 14-day reactor cycle.

The exhaust equipment includes a vacuum pump for purging sections of the system. It also includes the equipment necessary for controlling the operation of the compressor, isolating sections of the system for evacuation, sampling the gas in the storage tanks, and for emptying the storage tanks.

Helium pressurization equipment. - The binary gas lines (except those in the monitored exhaust equipment cabinet) that may contain radioactive gases are blanketed with helium. This is accomplished by introducing static helium into the annulus formed by a tube which has been installed over the binary gas line. The helium blanket is maintained at a pressure at least 15 percent higher than that in the inner line and that exterior to the outer jacket. The pressurization equipment consists of a standard high-pressure helium bottle, pressure regulators, and various valving and pressure gages.

## Control and Instrumentation

All the instruments of the experiment are installed in eight standard instrument bays. One bay is installed in the bottom of the dry annulus inside of the reactor containment vessel (fig. 3). The other seven bays are installed in the experiment control room (XCR) annex. Figure 9 shows four of the bays and is typical of the appearance


Figure 9. - Instrument console bays 1 to 4.

of all eight bays. The instruments have various functions including monitoring, alarm, control, and safety. The parameters monitored by the instruments are

(1) Fuel temperature
(2) Insulator temperature
(3) Insulator resistance
(4) Coolant water temperature
(5) Neutron flux
(6) Gamma flux
(7) Binary gas pressure
(8) Binary gas flow
(9) Binary gas storage pressure
(10) Binary gas radioactivity

The alarms that are actuated by the instrumentation are

(1) Binary gas supply bottle (low)

(2) Fuel pellet temperature (high)

(3) Water temperature (high)

(4) Compressor outlet pressure (high)

(5) Helium pressure (low)

(6) Argon pressure (low)

(7) Storage tank pressure (high)

(8) Binary gas pressure (low)

(9) Binary gas flow (low)

(10) Binary gas containment pressure (low)

(11) Direct-current voltage (low)

(12) Alternating-current voltage (low)

(13) Binary gas activity (high)

(14) Emergency helium flush

The only control function of the instrumentation is the binary gas control of the fuel temperature. The fuel temperature monitoring and control instrumentation is divided into three identical circuits, one for each capsule. A typical fuel temperature monitor-

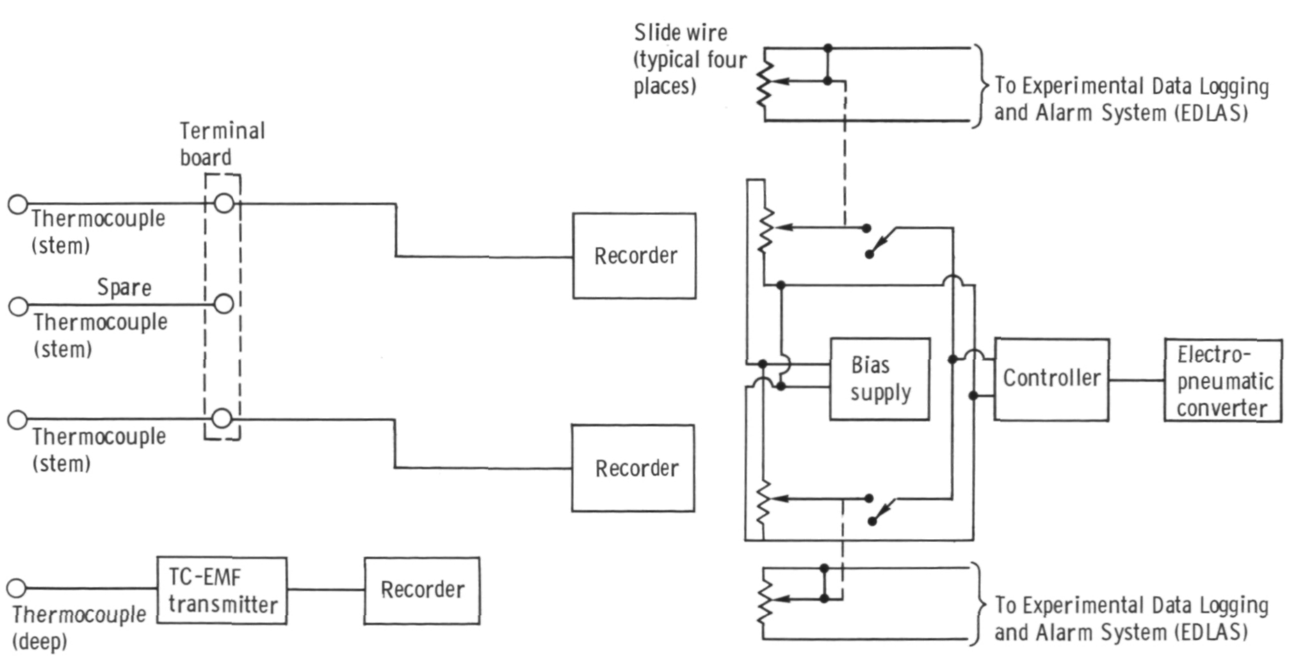


Figure 10. - Fuel specimen temperature control circuit.

ing and control circuit is shown diagrammatically in figure 10.

The fuel capsule is instrumented with four high-temperature, refractory metal thermocouples. One of these senses the temperature at the end of the fuel specimen. This thermocouple is referred to as the "deep" thermocouple. The other three thermocouples sense the temperature midway between the end of the fuel specimen and the end of the primary containment vessel. These thermocouples are referred to as the "stem" thermocouples.

The signal from the deep thermocouple is recorded on a strip-chart recorder and is not used in the control circuit. The control circuit uses the signal from two of the stem thermocouples. The third stem thermocouple is used as a spare. The signals from the stem thermocouples are recorded on two single-pen strip-chart recorders. Signals from retransmitting slide wires in the recorders are sent to the controller. A switching network enables the operator to choose which temperature signal is to be sent to the controller. The controller compares the temperature signal with a setpoint, and if there is a difference, the controller sends an error signal to the electropneumatic converter in the proportioning mechanism.

The safety functions of the instrumentation are all associated with high fuel specimen temperatures. They are initiated by limit switches on the stem temperature recorders. The sequence of functions as the stem temperature increases past successive limit switch settings is as follows:

(1) There is a high-temperature alarm.
(2) A slow reactor power setback is initiated.
(3) There is a helium flush through the capsule.
(4) The reactor is "scrammed."

## PRELIMINARY EXPERIMENT TESTS

Various tests were run to obtain design and analysis information and for checking the components and assemblies in the experiment. The thermocouple thermal cycling tests, control loop tests, and nuclear mockup tests, are discussed in appendixes A, B, and C, respectively. Other tests are described briefly in the following paragraphs.

### Thermal Mockup Test

The objective of the thermal mockup test was to establish the feasibility of controlling temperature with a binary gas. The mockup consisted of a resistance-type heater, the primary containment vessel of 90 percent tantalum - 10 percent tungsten, the secon-

dary containment vessel of 304 stainless steel, a water jacket, binary gas lines, and four thermocouple leads. Test results were compared with computer code calculations.

### Hydraulic Mockup Test

A mockup of the experiment in-pile section flow paths was constructed to determine the coolant water flow and distribution. Local water velocities in high heat flux regions and water velocities between the ends of the test capsules and spacers were also determined.

### Miscellaneous Tests

A mockup of the in-tank assembly was used to obtain assembly practice, to permit underwater handling practice of the experiment, and to permit remote handling practice in the hot laboratory.

The individual components and the experiment assembly were proof checked using resistivity measurements, pressure tests, X-ray radiography, and helium leak detection.

## HEAT-TRANSFER ANALYSES

Heat-transfer calculations were conducted to determine the heat removal requirements, peak operating temperatures, range of temperature control using a binary gas, and the postirradiation temperatures. The following sections summarize these calculations and their results.

### Heat Output and Coolant Temperature Rise

The principal heat sources in the experiment are fission heat, gamma heat from the reactor, and the heat generated in the neutron shield due to the cadmium $(n, \gamma)$ reaction and the boron-10 $(n, \alpha)$ lithium-7 reaction. The maximum total heat output of the experiment in-pile section is $5.23\times10^5$ Btu per hour (153.1 kW).

The experiment test section is cooled by the same primary coolant water flow that cools the reactor core. The water flows downward through the test hole. The water inlet temperature is $135^{\circ}$ F (330 K). There are two parallel coolant channels in the test

section. The maximum exit temperature of the inner channel is $160^{\circ}$ F (344 K). The maximum exit temperature of the outer channel is $173.5^{\circ}$ F (351 K).

## Fuel Capsule Temperature

It is planned to operate the three fuel specimens at clad hotspot temperatures of $2600^{\circ}$, $2870^{\circ}$, and $3140^{\circ}$ F (1700, 1850, and 2000 K). This is possible since the temperature of each fuel capsule is individually controlled. Figure 5 shows the geometry of a typical fuel capsule.

Water flows axially at the outer radius of the capsule and acts as a heat sink. There is a layer of water contained at each end between the stainless-steel and aluminum end pieces. The water at both ends has a radial velocity such as to provide a heat-transfer coefficient about one-third that along the outer radius due to axial flow. A layer of helium gas insulates the fuel clad from the inner containment vessel. An adjustable mixture of helium and argon provides temperature control and insulation between the two containment vessels.

A digital computer code (ref. 1) was used to calculate the fuel capsule temperatures. A large range of heating rates occurs in the experiment. The code input values include fission heats ranging from 5595 to 22 380 Btu per hour per cubic inch (100 to 400 $W/cm^3$) and gamma heats ranging from 6200 to 18 600 Btu per hour per pound (4 to 12 W/g). The binary gas composition (helium and argon) is varied through the entire range (zero to 100 percent helium).

The temperature profile for capsule 3 is presented in figure 11. Capsule 3 is operated at a clad hotspot temperature of $3140^{\circ}$ F (2000 K), the highest temperature of the three fuel capsules.

Clad hotspot temperatures of the fuel specimens are controlled by one of the three stem thermocouples of each fuel capsule. The relation of the stem thermocouple temperature, fuel end temperature, and helium fraction as a function of the reactor control rod bank height for capsule 2 is shown in figure 12. The clad hotspot temperature in capsule 2 is controlled at $2870^{\circ}$ F (1850 K). This capsule experiences the largest variation of heat generation (see appendix C). The stem thermocouple temperature varies from $2125^{\circ}$ to $2290^{\circ}$ F (1435 to 1528 K) during the reactor cycle. Thus, it is necessary to vary the setpoint of the controller with control rod bank height to maintain the clad hotspot temperature at $2870^{\circ}$ F (1850 K). Although the other fuel capsules experience lesser variations in heat generation, the necessity to vary their controller setpoints remains.

A preliminary analysis was made to determine the uncertainty in the clad hotspot temperature. The uncertainties associated with each of the heat-transfer parameters were statistically combined. The total uncertainty calculated is for two standard devia-

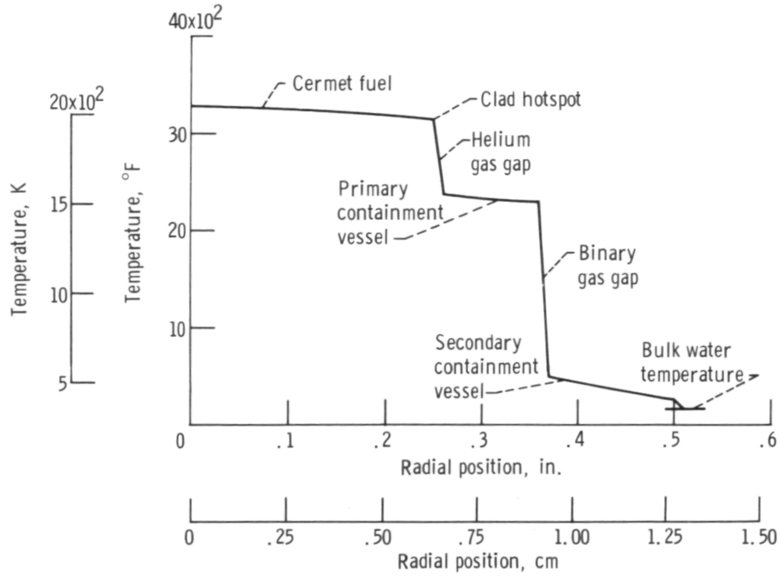


Figure 11. - Radial temperature profile at hotspot for capsule 3. Fission heating, 16 780 Btu per hour per cubic inch (300 W/cm$^3$); gamma heating, 13 950 But per hour per pound mass (9.0 W/g); binary gas, 84 percent helium - 16 percent argon.

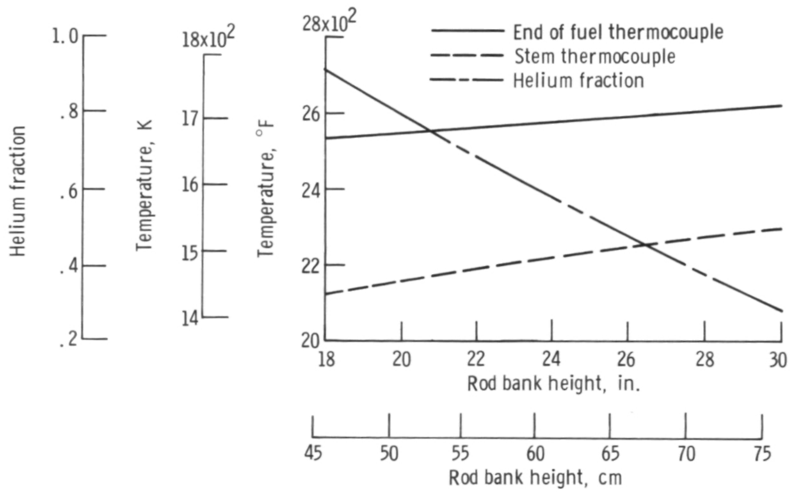


Figure 12. - Thermocouple temperatures and helium fraction as function of rod bank height for capsule 2. Fuel clad hotspot temperature, 2870° F (1851 K).

tions of the individual errors. This results in a 95-percent confidence level.

Four cases at the start of irradiation and two cases at the end of irradiation (3000 hr) have been studied. The results are summarized in table I.

This analysis is of a preliminary nature aimed at determining the maximum uncertainty that could occur in the experiment. This occurrence has a low probability. A detailed analysis will probably show that the maximum error for the controlled stem temperature case will be about $\pm 144^{\circ}$ F ($\pm 80$ K).

Table II summarizes the fuel capsule thermal conditions in the experiment.

TABLE I. - FUEL TEMPERATURE CONFIDENCE BANDS

| Case | Description | Clad hotspot temperature, $^{\circ}$F | Clad hotspot temperature, K |
|---|---|---|---|
| | Startup | | |
| I | Controlling on stem temperature | 3140±241 | 2000±134 |
| II | Controlling on fuel end (deep) temperature | 3140±204 | 2000±113 |
| III | Argon accident; 100 percent argon in binary gas | 5070±666 | 3074±370 |
| IV | 100 percent helium case | 3140±462 | 2000±257 |
| | End of irradiation | | |
| V | Controlling on stem temperature | 3140±570 | 2000±317 |
| VI | Argon accident | 5070±927 | 3074±515 |

TABLE II. - FUEL CAPSULE TEMPERATURES

| Capsule number | Gamma heating | | Fission power density | | Fuel centerline temperature | | Clad temperature | | Deep thermocouple temperature | | Stem thermocouple temperature | | Primary containment vessel hotspot temperature | | Secondary containment vessel hotspot temperature | |
|---|---|---|---|---|---|---|---|---|---|---|---|---|---|---|---|---|
| | Btu/hr-lb | W/g | Btu/hr-in.$^3$ | W/cc | $^{\circ}$F | K | $^{\circ}$F | K | $^{\circ}$F | K | $^{\circ}$F | K | $^{\circ}$F | K | $^{\circ}$F | K |
| Reactor control rod bank height, 18.0 in. (45.7 cm) | | | | | | | | | | | | | | | | |
| 2 | $12.55\times10^3$ | 8.1 | $13.43\times10^3$ | 240 | 2973 | 1907 | 2870 | 1850 | 2539 | 1666 | 2122 | 1434 | 2071 | 1406 | 246 | 392 |
| 3 | 13.63 | 8.8 | 14.55 | 260 | 3250 | 2061 | 3140 | 2000 | 2777 | 1798 | 2352 | 1562 | 2325 | 1547 | 253 | 396 |
| 4 | 7.90 | 5.1 | 6.44 | 115 | 2638 | 1721 | 2600 | 1700 | 2375 | 1575 | 2060 | 1400 | 2145 | 1447 | 207 | 370 |
| Reactor control rod bank height, 30.0 in. (76.3 cm) | | | | | | | | | | | | | | | | |
| 2 | $7.13\times10^3$ | 4.6 | $6.72\times10^3$ | 120 | 2941 | 1889 | 2870 | 1850 | 2617 | 1709 | 2291 | 1528 | 2469 | 1627 | 202 | 368 |
| 3 | 15.02 | 9.7 | 12.60 | 225 | 3255 | 2064 | 3140 | 2000 | 2825 | 1825 | 2428 | 1604 | 2357 | 1565 | 258 | 399 |
| 4 | 12.00 | 7.75 | 11.20 | 200 | 2689 | 1749 | 2600 | 1700 | 2323 | 1546 | 1933 | 1329 | 1832 | 1273 | 240 | 389 |

## Insulator Capsule Temperatures

Two insulator capsules can be tested in each lead tube. The insulator test specimens are heated by gamma heating and have no temperature control. Maximum temperature is limited to $2090^\circ$ F (1417 K) nominally by the sizing of heat paths.

An insulator capsule consists of an evacuated stainless-steel cylindrical enclosure containing the cylindrical trilayer insulation specimen, a columbium pin to which the trilayer specimen is welded, and associated instrumentation (fig. 6). The columbium pin is necked down on one end. The diameter and length of this end is sized to limit the maximum temperature of the insulation. The necked down end is brazed to one of the end caps of the containment enclosure. The main portion (70 percent or more) of the heat generated within the containment enclosure is conducted across this pin to the end cap. The remaining heat is transferred by radiation.

The gamma heat generation for the insulator capsules was determined by extrapolating the experimental data obtained from the mockup reactor tests (see appendix C). A one-dimensional heat-transfer calculation was conducted on the two insulator capsules. The heat generation, the diameter D of the necked down portion of the columbium pin, and the insulation temperatures are listed in table III.

TABLE III. - INSULATOR CAPSULE TEMPERATURES

| Capsule number | Capsule location[a] | | Pin diameter, D | | Reactor control rod bank height | | Heat generation | | Insulation temperature | |
|---|---|---|---|---|---|---|---|---|---|---|
| | in. | cm | in. | cm | in. | cm | Btu/hr-lbm | W/g | $^\circ$F | K |
| 1 | -13.9 | -35.3 | 0.266 | 0.674 | [b]18.0 | 45.7 | $10.1\times10^3$ | 6.52 | 2010 | 1373 |
| | | | | | [c]30.0 | 76.2 | 2.10 | 1.36 | 690 | 638 |
| 5 | +9.5 | +24.1 | 0.172 | 0.436 | 18.0 | 45.7 | $3.75\times10^3$ | 2.42 | 1410 | 1040 |
| | | | | | 30.0 | 76.2 | 7.75 | 5.00 | 2090 | 1421 |

[a]Plus sign denotes above reactor core midplane; minus sign denotes below reactor core midplane.
[b]Start of reactor cycle.
[c]End of reactor cycle.

## Neutron Shield Temperatures

The neutron shield surrounding the test capsules (fig. 13) is heated by gamma radiation from the reactor, the Cd(n, $\gamma$) reaction and the $B^{10}(n, \alpha)Li^7$ reaction. The neutron shield is cooled both at its inside and outside diameter by flow of primary coolant water.

After about 5000 hours irradiation, the cadmium is no longer effective in absorbing

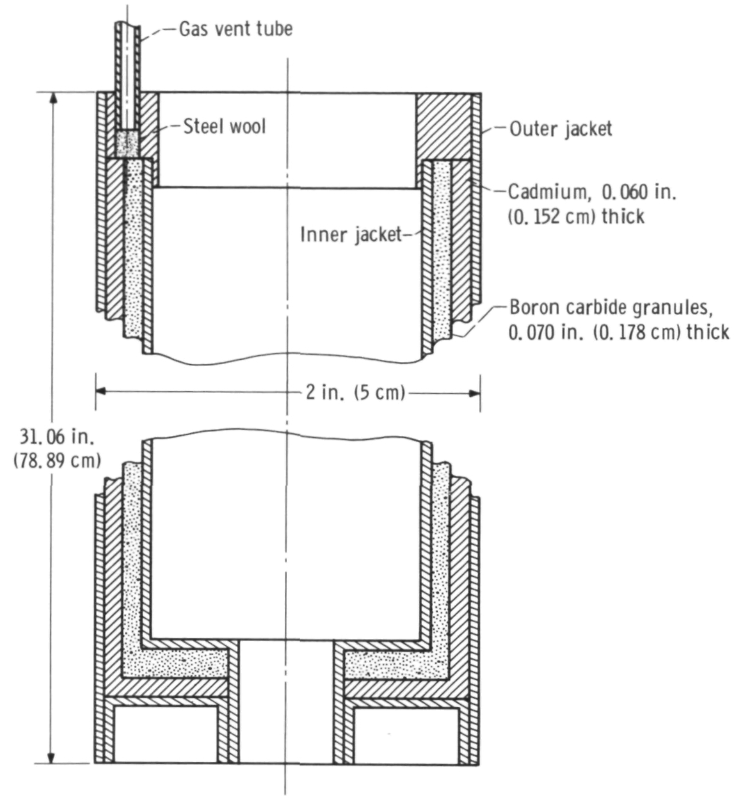


Figure 13. - Neutron shield.

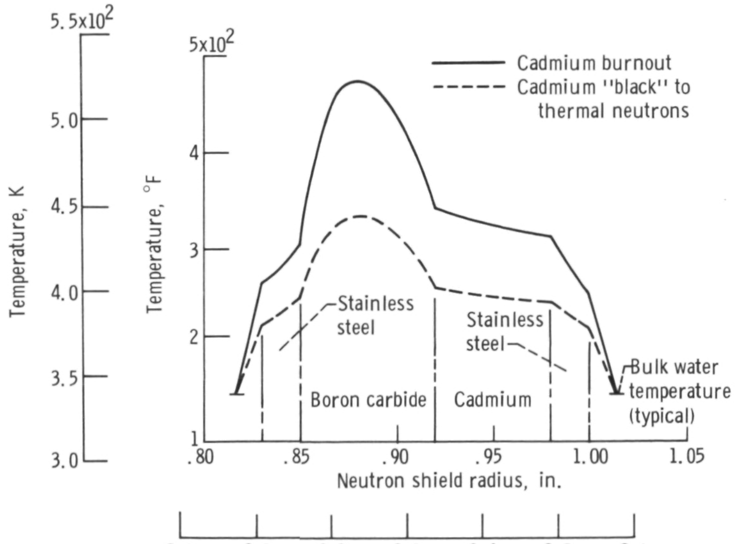


Figure 14. - Neutron shield temperature profile.

thermal neutrons. This cadmium ''burnout'' increases the heat generation in the boron carbide layer.

Figure 14 shows the peak radial temperature profile in the shield before and after cadmium burnout. The maximum temperature in the shield is 478° F (521 K). This temperature occurs in the boron carbide layer after cadmium burnout. The maximum cadmium temperature is 343° F (446 K).

## Postirradiation Temperatures

After irradiation, the experiment is transported underwater to the hot laboratory where it is disassembled in air. Since the primary containment vessels are made of the 90-percent-tantalum - 10-percent-tungsten alloy, the test section temperatures in air remain at relatively high levels for a long period of time after irradiation. This phenomenon results from production of the tantalum-182 isotope, which has a 115-day half-life. The activity in the test section associated with the tantalum-182 isotope is 12 800

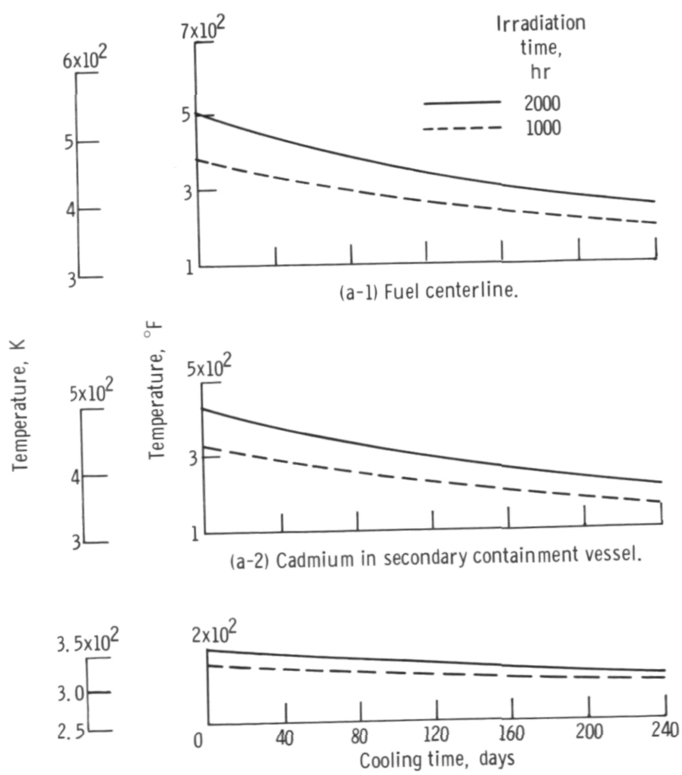

(a) With neutron shield in place.

Figure 15. - Capsule temperature in air.

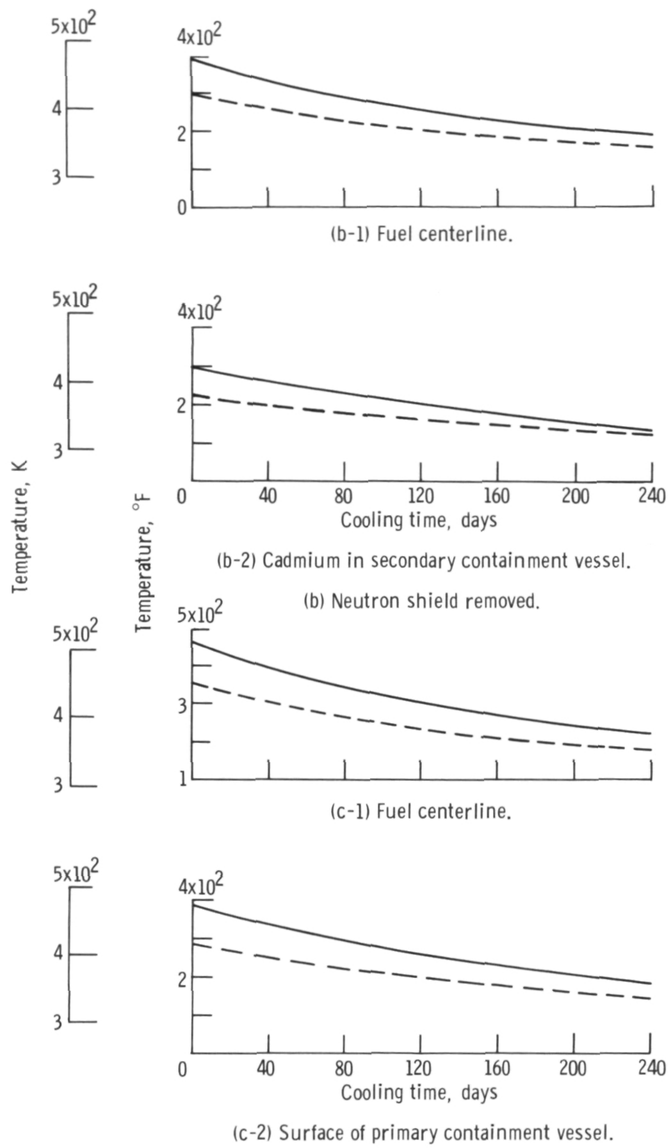


(c) Secondary containment vessel removed.

Figure 15. - Concluded.

and 25 900 curies ($4.7\times10^{14}$ and $9.6\times10^{14}$ dis/sec) for irradiation times of 2000 and 10 000 hours, respectively.

Postirradiation temperatures in the test section were calculated at various stages of disassembly. Figure 15 shows the temperatures of the fuel capsule in air as a function of cooling time after irradiation.

Cadmium melting does not occur up to an irradiation time of 2000 hours. However, the high surface temperatures may require special handling in the hot laboratory. The use of tantalum is also a disadvantage because it reacts with the impurities in the binary

control gas. Longer term tests will require a change of the primary containment vessel material.

## STRESS ANALYSIS

All experiment components have been designed in accordance with references 2 and 3. All pressure-containing components have been proof pressure tested at either 150 percent hydraulically or 125 percent pneumatically of the design pressure.

Helium from the $B^{10}(n, \alpha)Li^7$ reaction can internally pressurize the neutron shield. Buckling of the inner tube can be avoided if the pressure differential is less than 18.1 psi (11.5 $N/cm^2$) (ref. 2). For a 10-percent release of helium from the boron carbide, an internal pressurization rate of 0.2 psi per hour (0.138 $(N/cm^2)/hr$) occurs in an unvented shield. This required that the shield be vented. Thus, a vent line attached to the shield is routed to the exhaust gas equipment cabinet in the dry annulus where a pressure gage monitors the pressure in the shield. The internal shield pressure will be limited to 10 psig (6.9 $N/cm^2$ gage).

## NEUTRON SHIELD BURNUP

The effective lifetime of the cadmium layer in the neutron shield (fig. 13) was calculated to be 4500 hours. For this exposure time, the boron-10 burnup is 13.8 percent. With this depletion of boron-10, the fission heating rate in the fuel specimen increases 6 percent.

## TEST PROCEDURES

The general test procedures used in preparing, conducting, and completing an irradiation test are presented in the following paragraphs.

### Preirradiation Checkout

Two weeks prior to the installation of the in-tank assembly in the reactor tank, the control console and support equipment are checked out and all the instruments are calibrated. Following installation, a neutron shield leak test, electrical tests, and final system checkouts are conducted.

## Irradiation

At the start of the first reactor cycle, the reactor is held at the 30-megawatt power level while the fuel pins are brought up to temperature manually. After adjusting the controller sensitivity and switching the controllers to automatic, the control system response is checked by moving the setpoints downward 90 $F^{o}$ (50 K). At each additional 10 megawatts increase of reactor power, the control system stability is similarly checked until full reactor power (60 MW) is reached. Later experiment startups are conducted at the normal operating power levels of the reactor cycle.

During irradiation, all temperatures, gas flow, gas activity, neutron-gamma flux, and gamma flux are recorded on strip-chart recorders. Also, the experiment and reactor are protected by a reactor scram, a reactor setback, and alarms. An annunciator panel on the control console displays all off-normal conditions in the experiment. The events that cause a reactor scram are

(1) High fuel temperature (200 K above normal)
(2) Amplifier failure in a fuel temperature recorder
(3) Loss of thermocouple signal
(4) Loss of instrument power
(5) Loss of power to scram relays
(6) Loss of power to any pair of fuel temperature recorders

The experiment will cause a reactor slow setback in the event of

(1) High fuel temperature (150 K above normal)
(2) Thermocouple in control reading low
(3) Slow setback relays deenergized

Several alarm functions are available to indicate the occurrence of operational abnormalities in the experiment and support equipment.

In general, several reactor cycles are required to complete a planned irradiation test. Therefore, within 1 hour prior to a planned reactor shutdown, the temperature control system is switched to manual operation whereupon the control gas is changed to 100-percent helium. The gas flow is then shut off. This puts the experiment into a condition where it will not require surveillance during the reactor shutdown. While the reactor is being refueled, the experiment is removed from the LD-1 test hole and stored in a basket near the reactor tank wall. After refueling and replacement of the experiment in the LD-1 test hole, the neutron shield is leak tested.

## Transfer to Hot Laboratory

At the end of irradiation, the experiment is removed from the reactor tank, transported to the hot laboratory, disassembled and subjected to postirradiation examination.

The entire length of the in-tank assembly (fig. 4) is removed from the reactor tank. Prior to removal, the gas in the lines is sampled to determine its activity level. In the event of a high activity level, the gas lines are plugged and sealed in the junction box and on both sides of the filters. A transfer cap is installed over the exposed electrical leads and gas lines that were disconnected from the junction box. The cap is bolted to the top flange of the experiment lead assembly allowing underwater transfer. The experiment is then fed through the reactor fuel transfer chute into the water-filled quadrant C (fig. 3). The water shield surrounding the reactor facility and the water canals from the reactor to the hot laboratory are used for underwater transfer. In quadrant C, the experiment is coiled and secured to a transfer platform which is mounted on a remotely controlled underwater electrically powered vehicle. Figure 16 shows the mockup in-tank assembly secured to the transfer platform. The vehicle with the experiment is moved underwater through the canals to the hot handling room. The transfer platform is remotely removed from this canal and placed near the feed-through port at the rear of the hot cell (fig. 3). The in-pile section is then fed through the port into the hot cell where it is clamped in a fixture which remotely rotates and swivels the in-pile section to facilitate disassembly.

The radioactive experiment may be reinserted into the reactor for additional testing. If one or more fuel capsules are removed, aluminum spacers are assembled in their place, and the instrumentation leads and gas lines for the removed capsules are sealed. After installation of the neutron shield and leak testing, the experiment is transported

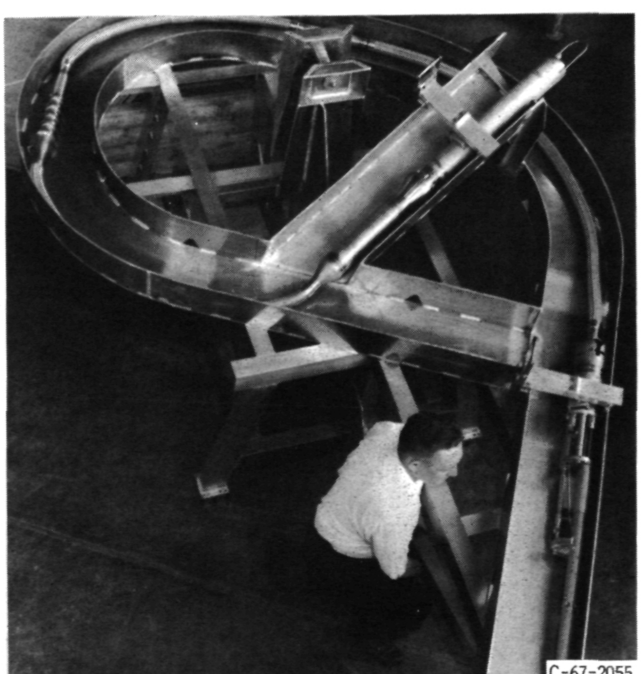


Figure 16. - Mockup in-tank assembly on transfer platform.

back to the reactor for continued irradiation of the remaining capsules. Transfer back to the reactor is essentially the reverse of the transfer to the hot laboratory.

## HAZARDS EVALUATION

Off-normal operating conditions of the experiment have been mentioned in the previous sections. The most serious failures, which may occur during a test, are presented, and the resulting conditions and safety actions associated with these failures are discussed.

### Experiment Maximum Credible Accident

The experiment maximum credible accident is an accidental insertion of 100-percent argon in the binary gas gap. The maximum fuel specimen clad hotspot temperature for this accident is $5070 \pm 927^{\circ}$ F ($3074 \pm 515$ K).

Although the hotspot temperature exceeds the melting point of uranium dioxide ($UO_2$) $4990^{\circ}$ F (3030 K), there is evidence that the fuel specimen may retain its shape. Tungsten - uranium dioxide cermets have been heated to $5440^{\circ}$ F (3273 K) for several minutes during brazing cycles (ref. 4). Excessive deformations or loss of $UO_2$ from the tungsten matrix does not occur during these brazing operations. These data do not prove that the fuel will not swell and will not release all fission gases. It may indicate, however, that the probability of fuel swelling, gas release, and rupture of the primary containment vessel is low.

If the primary containment is ruptured, 250 millicuries ($9.3 \times 10^{9}$ dis/sec) of fission gases could be released to the reactor containment vessel. Leaks from the exhaust gas equipment cabinet below the sensitivity of the RAMS radiation monitor can lead to this activity release. Local alarms will warn personnel of this hazard. Local evacuation of personnel from the dry annulus will be required.

The complete release of the maximum total fission gas activity (280 curies or $1.0 \times 10^{13}$ dis/sec) is not credible. This would require a simultaneous failure of a component in the exhaust gas equipment cabinet.

### Loss of Neutron Shield

There is a considerable buildup of lithium within the shield from the $B^{10}(n, \alpha)Li^{7}$ reaction. It is estimated that the $B^{10}$ atom burnup is approximately 31 percent for a 10 000-hour exposure. Lithium is very reactive with water, forming lithium hydroxide

and releasing considerable heat.

If primary water leaks into the neutron shield, the lithium-water reaction may take place at a fast enough rate to cause local melting of cadmium. The melted cadmium could then flow into the voids of the $B_4C$ allowing it to shift into the cadmium void. Such a shift could provide a direct path for streaming of thermal neutrons and a significant increase in the heat generation rate. The potential hazard of this accident is strongly dependent on the magnitude of the cadmium melting and subsequent shifting of the $B_4C$.

As a result of the void in the shield, thermal neutrons will impinge on the fuel capsules. Cadmium, in the walls of the secondary containment vessels of the fuel capsules, effectively shields the fuel test specimen from the major portion of these thermal neutrons. However, the fuel capsule ends are unshielded. This causes an increase in heat generation near the ends of the fuel test specimen. As a result, the peak temperature in the fuel could rise to only $3910^{\circ}$ F (2428 K) from a normal temperature of $3270^{\circ}$ F (2075 K). If the fuel capsules were unshielded by the cadmium in the secondary containment vessel wall, fuel meltdown would occur.

## Fission Gas Release

The release of fission gases from a fuel specimen to the primary water requires the rupture of the two experiment containment barriers as well as the fuel specimen cladding. Except for the maximum credible accident, only a primary water flow blockage at the entrance section near the top core grid plate could cause such extensive damage to all containment barriers. A rupture of all containment barriers of the three fuel specimen capsules could release 22 800 curies ($8.4\times10^{14}$ dis/sec) of mixed fission products to the primary water at the end of a 10 000-hour irradiation. This occurrence, however, is highly improbable since two independent events must take place: (1) a primary water flow blockage at the entrance section of the experiment and (2) a failure of the reactor setback.

A fission gas release to the exhaust system of the experiment can occur in the event of a control system malfunction, excessive heat generation rates in the fuel specimen, rupture of the specimen cladding, or primary water flow blockage. It is estimated that 22 800 curies ($8.4\times10^{14}$ dis/sec) of mixed fission product activity could be released to the secondary containment areas from the three fuel specimens. Only the fission gases could reach the exhaust system outside of the reactor tank. The activity of these gases is 280 curies ($1.0\times10^{13}$ dis/sec). The remaining fission products will condense and freeze on the walls of the secondary containment vessel within the reactor tank.

For a release of 280 curies ($1.0\times10^{13}$ dis/sec) to the exhaust equipment, the maximum total dose a person could receive is 152 mrad. This occurs if he is reading the pressure gages in the exhaust gas equipment cabinet located in the dry annulus.

# FUTURE ADAPTATIONS OF EXPERIMENT

The experiment was installed in the Plum Brook Reactor Facility and preliminary tests have been started. The performance of the experiment has met all its design objectives.

The use of a variable thermal conductivity gas for temperature control may be applied to other irradiation experiments. For a 0.010-inch- (0.25-mm-) thick layer of gas at an average temperature of $1110^{\circ}$ F (872 K), a thermal heat flux variation from 48 600 to 378 000 Btu per hour per square foot (15.4 to 119 $W/cm^2$) can be accommodated by varying the gas mixture from argon to helium. Heat fluxes in thermionics related experiments are in the range of 95 000 to 350 000 Btu per hour per square foot (30 to 110 $W/cm^2$). And temperatures are in the range of $1340^{\circ}$ to $3140^{\circ}$ F (1000 to 2000 K). Thus, a binary gas temperature control system is usable.

A vented external type thermionic fuel test specimen with binary gas temperature control is shown schematically in figure 17. The binary gas is shown between the primary and secondary containment inner tubes. A static gas of argon or neon between the fuel clad and the primary containment tube provides a temperature difference of about $1800^{\circ}$ F (1000 K) between these components to limit the containment temperature to $1200^{\circ}$ F (922 K). The reason for limiting the containment temperature to $1200^{\circ}$ F (922 K)

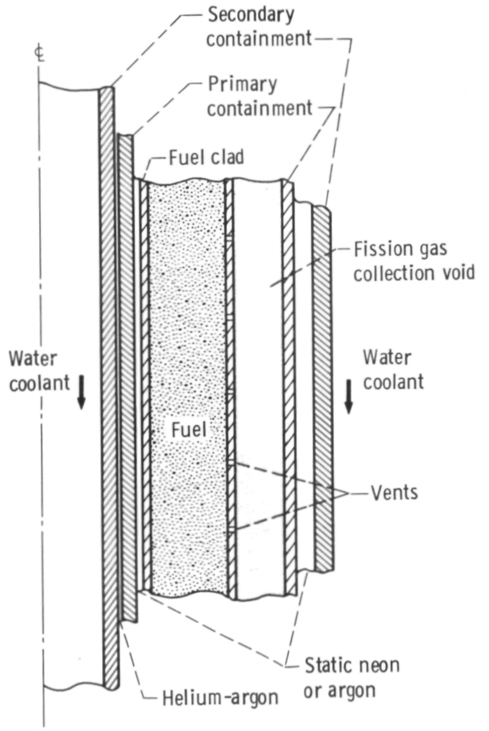


Figure 17. - Externally fueled and vented thermionic fuel test specimen with binary gas temperature control.

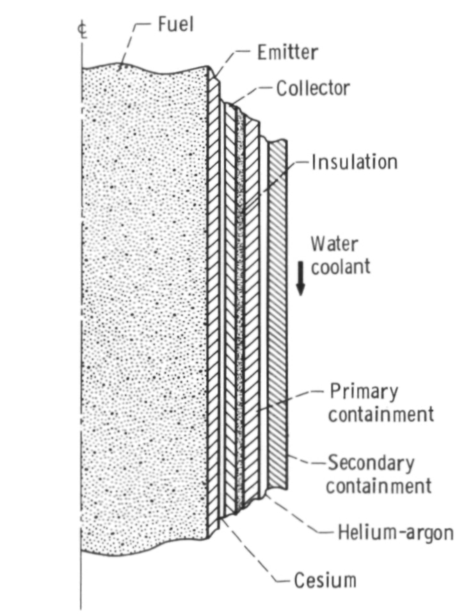


Figure 18. - Thermionic diode in-pile test with collector temperature control using binary gas.

is that stainless steel, which does not require high purity control gases, can be used.

An internally fueled thermionic diode is shown schematically in figure 18. The collector temperature can be controlled with a thin layer of the variable binary gas between the collector and the water coolant tube. Emitter temperature control can be accomplished by varying the electrical load resistance between the emitter and collector.

Lewis Research Center,
National Aeronautics and Space Administration,
Cleveland, Ohio, May 9, 1969,
120-27-05-03-22.

# APPENDIX A

## THERMOCOUPLE THERMAL CYCLING TESTS

The objective of this test was to qualify swaged tantalum sheathed tungsten against tungsten-rhenium thermocouples for the experiment under thermal cycling conditions.

Two types of thermocouples were tested: tungsten against tungsten - 25 percent rhenium and a doped tungsten against tungsten - 25 percent rhenium. Both types of thermocouples were thermal cycled 130 times from $260^{\circ}$ to $3140^{\circ}$ F (400 to 2000 K), and both types operated satisfactorily throughout the tests. Also, both types appear to be satisfactory from the thermal cycling standpoint for this experiment application.

### Thermocouple Description

Two types of high-temperature thermocouples are available for use in the experiment: tungsten against tungsten - 25 percent rhenium and a doped tungsten - 3 percent rhenium against tungsten - 25 percent rhenium. These thermocouples have tantalum sheaths 0.062 inch (0.158 cm) in diameter. The sheath wall is 0.010 inch (0.025 cm) thick. The insulation is vitrified beryllium oxide. The two thermocouple wires are 0.010 inch (0.025 cm) in diameter. A grounded junction is used. The junction is formed by wedging the thermocouple wires between a tantalum end plug and the sheath and sealed by tungsten inert gas welding.

### Test Equipment

The thermocouple thermal cycling apparatus (fig. 19) consists of a pneumatic actuator which provides a linear stroke, a vacuum seal mounted in the support flange which permits linear or rotary motion, a water-cooled area below the flange, and T-shaped radiation shields. A thermocouple is shown mounted in the apparatus and is in the inserted position.

The thermocouple thermal cycling apparatus is mounted in a resistance-heated vacuum furnace. Thermal cycling is accomplished by a timer which switches air to the pneumatic actuator, thereby inserting the tip of the thermocouple into the hot zone of the furnace or retracting it behind the radiation shields and into the water-cooled region of the apparatus. The output of the thermocouple is continuously recorded on a strip-chart recorder.

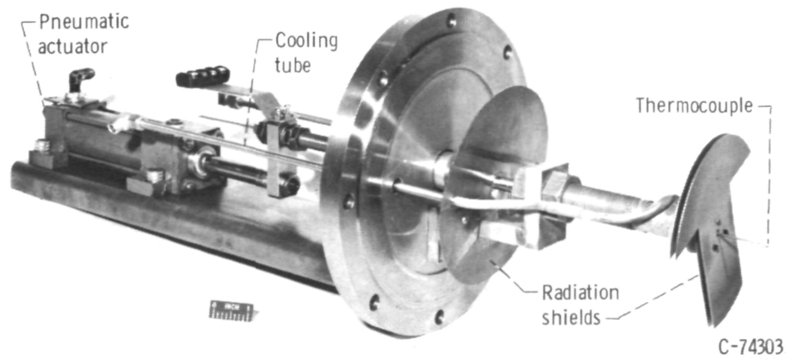


Figure 19. - Thermocouple thermal cycling apparatus.

## Test Procedure

Each thermal cycle consisted of a 45-second heatup time and a 5-minute cooldown time. The thermocouple is heated to a temperature of $3140^{\circ}$ F (2000 K) during the heatup and cooled to less than $260^{\circ}$ F (400 K) during the cooldown portion of the cycle. A portion of the temperature trace from the thermal cycling of a thermocouple is shown in figure 20.

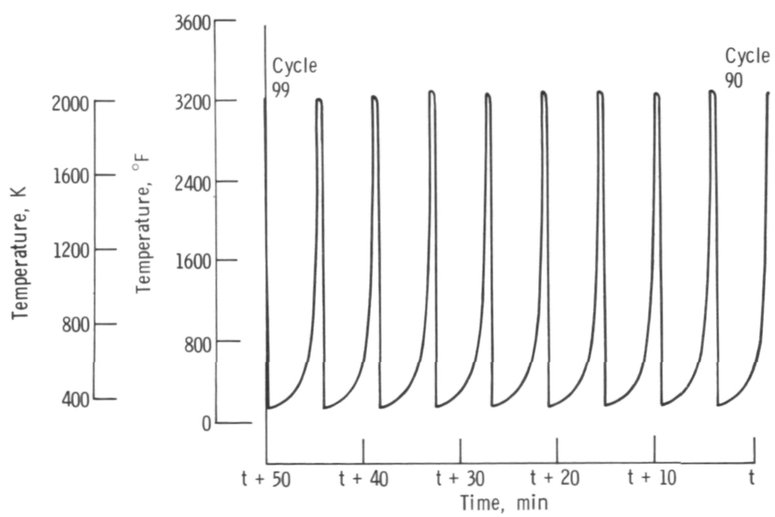


Figure 20. - Thermocouple temperature as a function at time during thermal cycling.

## Results

Both types of thermocouples were thermal cycled 100 times, soaked at $3140^{\circ}$ F (2000 K) for 50 hours, and thermal cycled again 30 to 50 times. Both types operated satisfactorily throughout the testing and calibrated properly in accordance with the specification in spite of a badly deteriorated tantalum sheath. The more severe deterioration of the tantalum sheath is shown in figure 21. This deterioration was caused by the introduction of water vapor into the vacuum furnace from a leak which developed in the cooling tube mounted on the cycling apparatus (fig. 19). This type of sheath failure is not expected to occur in the experiment. The void between the thermocouple sheath and thermocouple well in the experiment is filled with a static gas mixture of helium and argon. This gas will contain less than 1 ppm each of oxygen, nitrogen, and water.

Both types of thermocouples appear to be satisfactory from the thermal cycling standpoint for this experiment application.

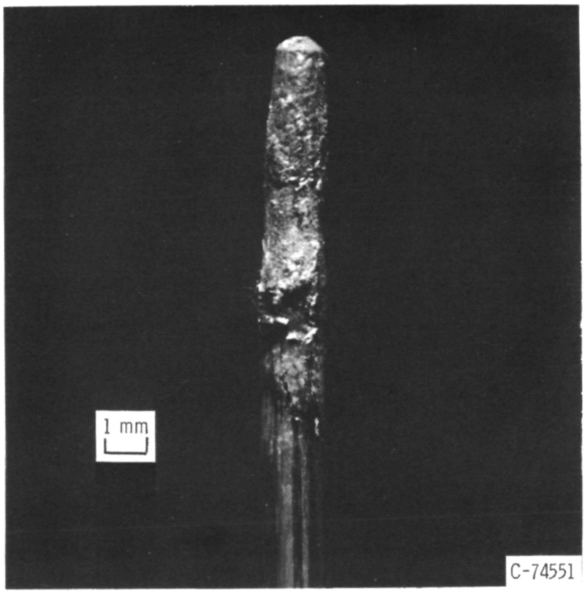


Figure 21. - Deteriorated thermocouple after thermal cycling test.

# APPENDIX B

## CONTROL LOOP TESTS

The objective of these tests were to determine and adjust the transient response and stability of the control loop for a step change in power at various gas supply pressures and power levels.

The stability of the control loop was tested by subjecting it to 20-percent step changes in power. This was done for gas pressures in the range 40 to 65 psig (27.6 to 44.9 $N/cm^2$ gage). The tests demonstrated that the controllers can be adjusted to keep the fuel temperature stable for these input conditions.

### Test Apparatus

The thermal mockup test apparatus (see section PRELIMINARY EXPERIMENT TESTS) was used as the heat source to test the control loop.

The electrical portion of the experiment control loop as installed in the instrument console was used for the thermal mockup control loop. Four thermocouples on the thermal mockup primary containment vessel were used as the basis for control.

The mechanical portion consisted of high-pressure bottles of argon and helium, pressure regulator valves, mass flow sensors, proportioning valves, 75 feet (22.9 m) of 0.022-inch (0.056-cm) inside-diameter tubing from the proportioning valves to the thermal mockup, and miscellaneous shutoff valves and piping. The components used were borrowed from the experiment control loop or were spares.

### Test Conditions

The temperature of the primary containment vessel was limited to a maximum of $1880^{\circ}$ F (1300 K) to extend the life of the resistance heater in the thermal mockup. The power was limited to 2660 Btu per hour (780 W) for the major portion of the testing. The power was increased to 3750 Btu per hour (1100 W) to determine the effect of power level on the control stability.

A 20-percent step change in power (increase or decrease) was applied to the heater, and the stability and response of the control system was observed. The maximum deviation of the temperature from the setpoint and the time required to return to the setpoint were the parameters used to measure the loop response. Instability of the control was determined from temperature oscillations. The stability and response of the control

TABLE IV. - OPTIMUM CONTROLLER SETTINGS

| Fuel capsule | Proportional band, percent | Reset rate, repeats/min | Helium pressure | | Argon pressure | |
|---|---|---|---|---|---|---|
| | | | psig | $N/cm^2$ gage | psig | $N/cm^2$ gage |
| 2 | 10 | 1.5 | 40 or 60 | 27.6 or 41.4 | 40 or 60 | 27.6 or 41.4 |
| 3 | 20 | | 40 or 60 | 27.6 or 41.4 | 40 or 60 | 27.6 or 41.4 |
| 4 | 20 | | 40 or 60 | 27.6 or 41.4 | 40 or 60 | 27.6 or 41.4 |
| 2 | 35 | | 40 | 27.6 | [a]45 | 31.1 |
| 3 | 75 | | 40 | 27.6 | [a]45 | 31.1 |
| 4 | 150 | | 40 | 27.6 | [a]45 | 31.1 |
| 2 | 20 | | 60 | 41.4 | [b]65 | 44.9 |
| 3 | 35 | 1.4 | 60 | 41.4 | [b]65 | 44.9 |
| 4 | 125 | 4.0 | 60 | 41.4 | [b]65 | 44.9 |

[a]Control is stable with argon pressure varied from 38 to 45 psig (26.2 to 31.1 $N/cm^2$ gage).

[b]Control is stable with argon pressure varied from 58 to 65 psig (40.0 to 44.9 $N/cm^2$ gage).

loop was determined for various gas pressures (see tables IV and V).

The behavior of the control loop was also determined for the case of an open-circuited input signal to the controller which is reestablished after some time.

## Control Loop Settings and Response

The controllers used in the experiment achieved automatic control by three actions, namely "proportional" action, "reset" action, and "rate" action. These actions are independently adjustable on each controller. The proportional action can be varied over a band from zero to 325 percent. The reset action is adjustable over a range from 0.02 to 100 repeats per minute. The rate action is adjustable over a range from zero to 8 minutes.

The control loop is tuned by determining the proportional, reset, and rate settings which will minimize the temperature deviation and response time for sudden changes in thermal power. This occurs with the most sensitive setting at each action. The maximum sensitivity of the system occurs with the narrowest proportional band, the highest reset range, and the lowest rate time. However, too high a sensitivity results in an unstable control system and temperature oscillations. A proportional band setting that is too narrow results in temperature oscillations of about 3 cycles per minute. A reset rate setting that is too high results in temperature oscillations of 2 cycles per minute. Instability did not develop with the rate at zero, the highest sensitivity for this function.

TABLE V. - SYSTEM RESPONSE FOR 20-PERCENT POWER CHANGE

| Fuel capsule | Helium pressure | | Argon pressure | | Controller settings | | Temperature deviation | | Recovery time, min |
|---|---|---|---|---|---|---|---|---|---|
| | psig | $N/cm^2$ gage | psig | $N/cm^2$ gage | Proportional band, percent | Reset rate, repeats/min | $F^o$ | K | |
| 2 | 40 | 27.6 | 40 | 27.6 | 10 | 1.5 | 81 | 45 | 2 |
| | | | 45 | 31.1 | 35 | 1.5 | 90 | 50 | 2 |
| | | | 40 | 27.6 | 35 | 1.5 | 153 | 85 | 5 |
| | 60 | 41.4 | 60 | 41.4 | 10 | 1.5 | 54 | 30 | 1 |
| | | | 65 | 44.9 | 20 | 1.5 | 54 | 30 | 1 |
| | | | 60 | 41.4 | 20 | 1.5 | 81 | 45 | 2 |
| 3 | 40 | 27.6 | 40 | 27.6 | 20 | 1.5 | 90 | 50 | 2 |
| | | | 45 | 31.1 | 75 | 1.5 | 81 | 45 | 2 |
| | | | 40 | 27.6 | 75 | 1.5 | 99 | 55 | 3.5 |
| | 60 | 41.4 | 60 | 41.4 | 29 | 1.5 | 72 | 40 | 1 |
| | | | 65 | 44.9 | 35 | 1.5 | 45 | 25 | 1 |
| | | | 60 | 41.4 | 35 | 1.5 | 99 | 55 | 2 |
| 4 | 40 | 27.6 | 40 | 27.6 | 20 | 1.5 | 72 | 40 | 2 |
| | | | 45 | 31.1 | 150 | 1.5 | 86 | 48 | 2 |
| | | | 40 | 27.6 | 150 | 1.5 | 144 | 80 | 5 |
| | 60 | 41.4 | 60 | 41.4 | 20 | 1.5 | 45 | 25 | 1 |
| | | | 65 | 44.9 | 125 | 4.0 | 45 | 25 | 1 |
| | | | 60 | 41.4 | 125 | 4.0 | 90 | 50 | 2 |

The optimum settings on the controller are defined as the most sensitive settings which can be used without causing instability. The best response occurs when the helium and argon pressures are equal because the proportional and reset actions can be set at more sensitive settings. The sensitivity of these actions must be reduced to maintain stability if the helium and argon are at different pressures. The optimum controller settings are listed in table IV for various helium and argon pressures.

The control loop response was evaluated by subjecting it to a 20-percent step change in power. The deviation of temperature from the setpoint and the time required to return to the setpoint were selected as the parameters of merit. Values of these parameters for various gas pressures and controller settings are listed in table V.

Figure 22(a) shows a typical trace of temperature against time for a 20-percent step change in power. And figure 22(b) shows a typical trace of temperature against time for a 90 $F^o$ (50 K) setpoint change. These curves were made with a 20-percent

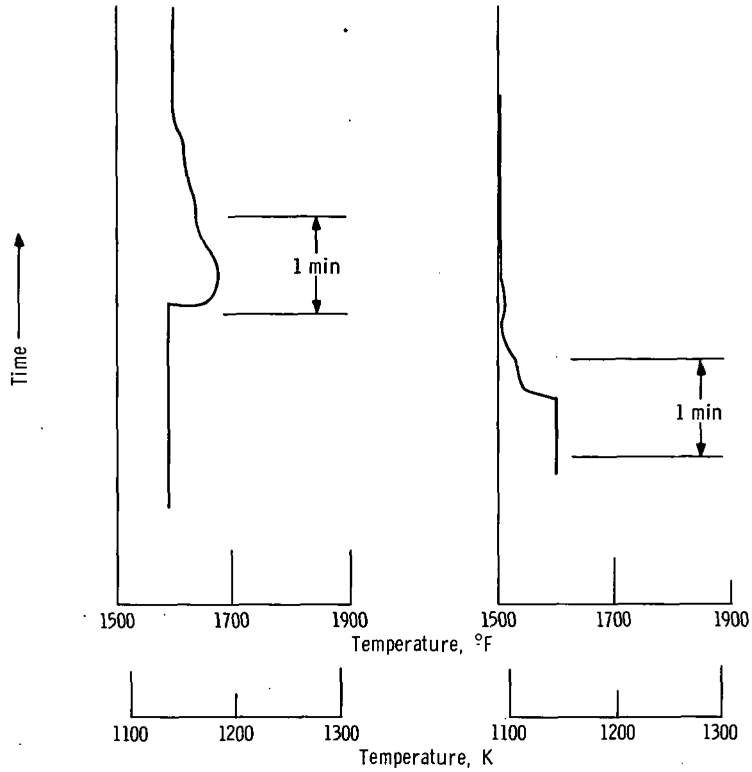


(a) 20-Percent step change in power.

(b) 90 F° (50 K) change of setpoint.

Figure 22. - System response for 60 psig (41.4 N/cm$^2$ gage) helium and argon supply with a 20-percent proportional band and a reset rate of 1.5 repeats per minute.

proportional band, a reset rate of 1.5 repeats per minute, and with the helium and argon supply pressures at 60 psig (41.4 N/cm$^2$ gage).

Additional testing was done at 3750 Btu per hour (1100 W). In order to maintain stability at the higher power, it was necessary to increase the proportional bandwidth slightly.

The tests demonstrated that the controllers can be adjusted to keep the control loop stable for almost any input condition.

# APPENDIX C

## FISSION AND GAMMA HEAT GENERATION AS MEASURED IN THE MOCKUP REACTOR

The objectives of this test were to determine experimentally the fission and gamma heat generation rates in the fuel test capsules when being irradiated in the LD-1 test site of the Plum Brook Reactor Facility, to measure the fast flux, and to determine the reactivity worth of the experiment.

A mockup of the in-pile section was inserted into the LD-1 test site of the Plum Brook Reactor Facility Mockup Reactor. Gamma heat generation was measured by sulfate-type dosimeters. Fission heating was measured by uranium-235 foil activation. The gamma and fission heating data have a two-sigma uncertainty (two standard deviations) of ±30 percent.

Fission heating was determined for two boron carbide ($B_4C$) thicknesses. This permitted the selection of a $B_4C$ thickness that would result in the desired level of fission heating. A $B_4C$ thickness of 0.070 inch (0.178 cm) with a $B_4C$ density 65 percent of theoretical density was selected.

Fast flux measurements were made by irradiating uranium-238 and neptunium-237 foils. The reactivity worth of the in-pile section is a negative 41.6 cents.

Thermal neutron effects in the fuel specimens are minimized by cadmium shielding. The effects of low-energy, epithermal neutrons are reduced by shielding with the $B^{10}$ isotope in the form of $B_4C$. The fission heat generation rate for such an experiment cannot be calculated accurately because of a lack of information on neutron flux and energy spectrum. It was therefore decided that the heat generation rates would be determined experimentally. The desired peak total heat generation (fission + gamma) in the fuel is 22 400 Btu per hour per cubic inch (400 W/cc). To attain this total heat generation, the thickness of $B_4C$ in the shield is varied in the mockup reactor test to adjust the fission heat component.

### Description of Equipment

All testing was performed in the mockup reactor. Both foil activation (neutron flux) and gamma heating measurements can be made in the mockup reactor when it is operating at a power level of 10 to 100 kilowatts. The data obtained in the mockup reactor must be scaled up to the Plum Brook reactor operational power level.

A mockup of the in-pile section was constructed for testing in the mockup reactor. The mockup is schematically shown in figure 23. It consists of a neutron shield, three

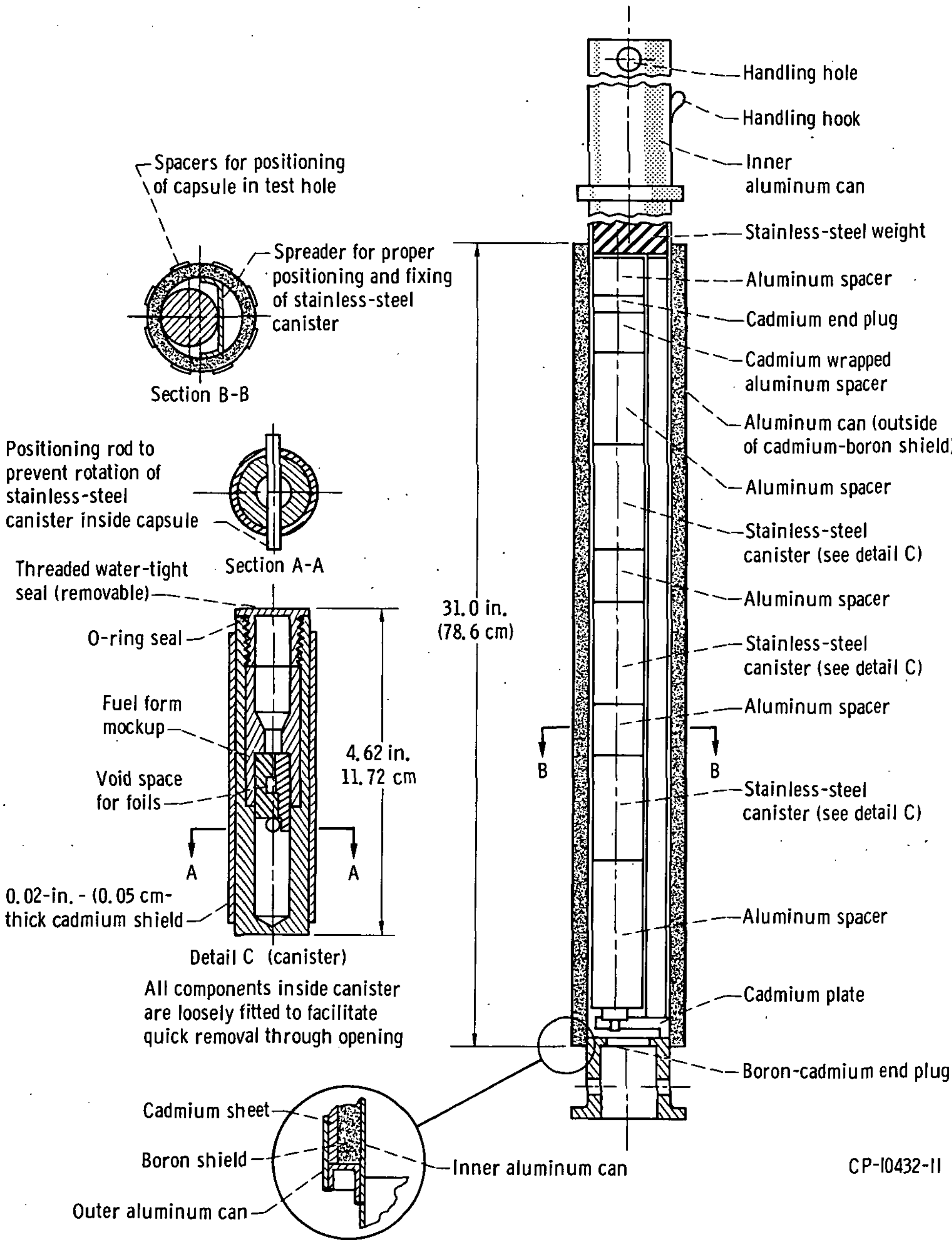


Figure 23. - In-pile section mockup for mockup reactor tests.

canisters simulating the fuel capsules, aluminum spacers, end shields, and suitable structure for positioning the test specimens and for handling purposes. The radial neutron shield is made up of concentric aluminum tubes welded into a leak-tight assembly. The annulus is filled with an outer layer of cadmium having a radial thickness of 0.035 inch (0.089 cm) and an inner layer of sintered particles of $B_4C$ enriched in the $B^{10}$ isotope to 92.3 percent.

Two shields were constructed to determine the effects of $B_4C$ radial thickness on fission heating. The $B_4C$ radial thicknesses were 0.117 and 0.055 inch (0.297 and 0.140 cm) with densities of 0.048 and 0.043 pound per cubic inch (1.33 and 1.19 g/cm$^3$), respectively, for these shields.

The fuel specimens and spacers are eccentrically located within the annular shield toward the core of the mockup reactor by a rib extending the full length of the shield. This is shown in section BB of figure 23. The fuel capsule consists of a type 304 stainless-steel canister which simulates the secondary containment vessel of the fuel capsule and a 90-percent-tungsten - 6-percent-copper - 4-percent-nickel specimen holder which simulates the primary containment vessel and the fuel. The fuel specimen used to determine heat generation rates is a thin disk of fully enriched (92.3 percent) $U^{235}$ foil. Through the use of pins and flats, the fuel specimen is oriented so that its flat face is parallel to the core.

## Test Procedures

Mockup reactor testing of the in-pile section mockup determined fission heating, fast neutron flux, and the reactivity worth of this experiment. The dosimetry methods used in conjunction with the mockup reactor to determine these parameters are fully described in section V of the "Standard Guides to the Design of Experiments for the Plum Brook Reactor Facility" (by the Staff of the PBRF, Feb. 8, 1965). A listing of the methods and procedures used is included herein.

The fission rate was determined by nondestructive counting of the lanthanum-140 isotope in the irradiated $U^{235}$ foils. The number of fissions was also determined by destructive radiospectrographic methods. The gamma heating ratio was determined through the use of standard Fricke ferrous sulfate dosimeters. Fast flux measurements were made by irradiating $U^{238}$ and $Np^{237}$ foils. Perturbation of thermal flux at adjacent test sites was determined from gold- and cadmium-covered gold foils irradiated with and without the in-pile section mockup in the mockup reactor. The reactivity worth was determined by the criticality change of the mockup reactor with the in-pile section mockup installed.

# Results

The gamma and fission heating were determined in the LD-1 test site at three vertical locations and three control rod bank height positions.

The gamma heating results are shown in figure 24. The gamma heating is seen to vary with test position and rod bank height. Test specimens in the upper portion of the core (capsule 4) will experience an increasing gamma heating over the Plum Brook Reactor fuel cycle. Test specimens near the core centerline (capsule 3) experience a slight increase in gamma heating over the reactor cycle. Test specimens in the lower portion of the core (capsule 2) will experience a decreasing gamma heating over the reactor cycle.

The maximum fission heating rates with the Plum Brook Reactor power at 60 megawatts were 12 300 and 19 600 Btu per hour per cubic inch (220 and 350 $W/cm^3$) for the 0.117- and 0.055-inch- (0.297- and 0.139-cm-) thick $B_4C$ shields, respectively. The maximum desired fission heating is 15 060 Btu per hour per cubic inch (269 $W/cm^3$). This maximum fission heating can be attained by interpolating the test results which required that $\rho_x$ = 0.00415 pound per square inch (0.292 $g/cm^2$), where $\rho$ is the density and x is the thickness of $B_4C$ in the neutron shield. The final shield, as fabricated for

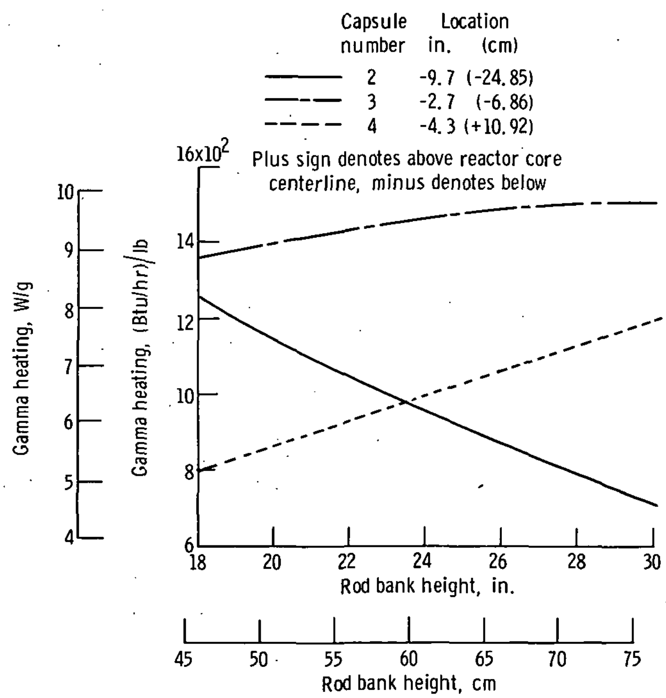


Figure 24. - Gamma heating against reactor control rod bank height. Reactor power, 60 megawatts; test site, LD-1; neutron shield: cadmium, 0.06 inch (0.152 cm); boron carbide, 0.07 inch (0.178 cm).

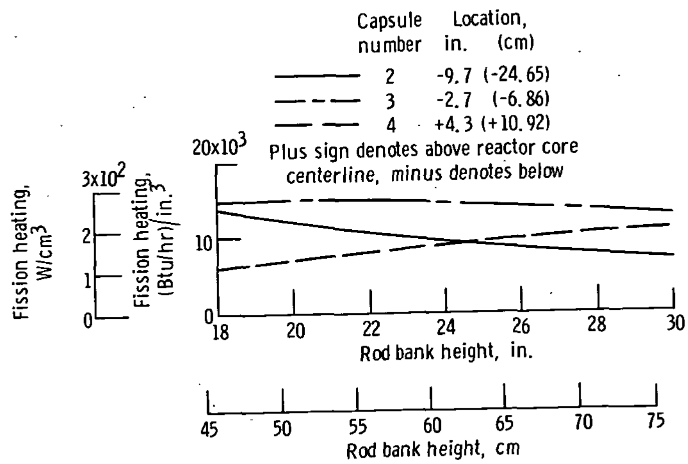


Figure 25. - Fission heating against reactor control rod bank height. Reactor power, 60 megawatts; test site, LD-1; neutron shield: cadmium, 0.06 inch (0.152 cm); boron carbide, 0.07 inch (0.178 cm).

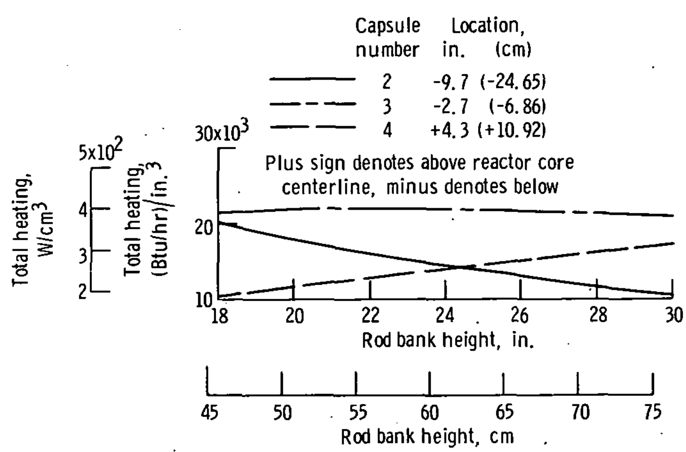


Figure 26. - Total heating against reactor control rod bank height. Reactor power, 60 megawatts; test site, LD-1; neutron shield: cadmium, 0.06 inch (0.152 cm); boron carbide, 0.07 inch (0.178 cm).

the experiment, had an average $B_4C$ density of 0.0592 pound per cubic inch (1.64 $g/cm^3$), a $B_4C$ radial thickness of 0.070 inch (0.178 cm), and a cadmium radial thickness of 0.060 inch (0.152 cm).

The fission heat generation shown in figure 25 varies in a manner similar to gamma heating. The total heating for the test specimen is shown in figure 26.

Figure 27 illustrates the variation of fission heating with $B_4C$ thickness $x$ and density $\rho$ at the core centerline of LD-1 for the startup condition which consists of a 15.4-inch (39.12-cm) reactor control rod bank height and a reactor power of 40 megawatts.

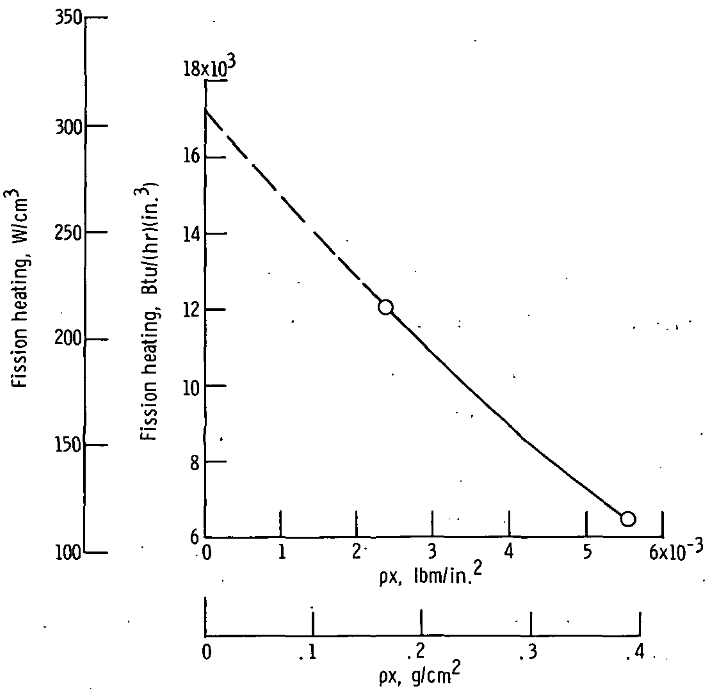


Figure 27. - Variation of fission heating with boron carbide shield thickness and density at core centerline. Reactor power, 40 megawatts; test site, LD-1; rod bank height, 15.4 inches (39.12 cm). Boron carbide is 92.3 percent enriched in $B^{10}$ isotope. Fuel composition, 50-volume-percent-$UO_2$ - 50-volume-percent-W cermet. $UO_2$ is 92.3 percent enriched in $U^{235}$ isotope.

The data are extrapolated to zero $B_4C$ thickness where the value of fission heating was analytically estimated on the basis of flux transmission factors. An estimate of the fission heating for various shield thicknesses at other positions in the LD-1 test hole, at 60 megawatts reactor power and at other control rod bank heights, can be made by normalizing the data of figure 27 to that of figure 25. Table VI(a) presents the fast flux greater than 0.75 MeV for three vertical locations in the LD-1 test site and for three rod bank height positions. Table VI(b) presents fast flux greater than 1.45 MeV for this site, vertical locations, and rod bank height positions. All data are for a 0.070-inch (0.178-cm) $B_4C$ shield and a Plum Brook reactor power of 60 megawatts. The fast flux measured was internal to the secondary containment vessel.

The experiment is black to thermal neutrons. The reactivity worth of the experiment as measured in the mockup reactor is a negative 41.6 cents.

TABLE VI. - FAST FLUX FOR EXPERIMENT IN LD-1 TEST

SITE OF PLUM BROOK REACTOR

[Reactor power, 60 MW; boron shield thickness, 0.070 in. (0.178 cm).]

(a) Greater than 0.75 MeV

| Vertical location relative to core centerline[a] | | Rod bank height, in. (cm) | | |
|---|---|---|---|---|
| | | 18.0 (45.7) | 24.0 (60.9) | 30.0 (76.3) |
| in. | cm | Fast flux, neutrons/($cm^2$)(sec) | | |
| +4.3 | +10.9 | $2.1\times10^{13}$ | $2.6\times10^{13}$ | $3.6\times10^{13}$ |
| -2.7 | -6.9 | 5.1 | 5.3 | 5.4 |
| -9.7 | -24.4 | 4.5 | 3.1 | 2.4 |

(b) Greater than 1.45 MeV

| | | | | |
|---|---|---|---|---|
| +4.3 | +10.9 | $0.8\times10^{13}$ | $1.5\times10^{13}$ | $2.6\times10^{13}$ |
| -2.7 | -6.9 | 2.4 | 2.6 | 2.5 |
| -9.7 | -24.4 | 3.9 | 2.3 | 1.3 |

[a]Plus sign denotes above core centerline, minus sign denotes below.

## REFERENCES


1. Mollerus, F. J., Jr.: Steady State Heat Transfer Program (STHTP). Rep. HW-73668, Hanford Lab., General Electric Co., May 12, 1962.
2. Anon.: ASME Boiler and Pressure Vessel Code. Section III, Nuclear Vessels. 1963.
3. Anon.: ASME Boiler and Pressure Vessel Code. Section VIII, Unfired Pressure Vessels. 1965.
4. Moore, Thomas J.; and Adams, Donald W.: A Procedure for Furnace Brazing Butt Joints in Tungsten - Uranium Dioxide Cermet Cylinders at $3000^{\circ}$ C. NASA TM X-1815, 1969.

*"The aeronautical and space activities of the United States shall be conducted so as to contribute . . . to the expansion of human knowledge of phenomena in the atmosphere and space. The Administration shall provide for the widest practicable and appropriate dissemination of information concerning its activities and the results thereof."*

— NATIONAL AERONAUTICS AND SPACE ACT OF 1958

# NASA SCIENTIFIC AND TECHNICAL PUBLICATIONS

TECHNICAL REPORTS: Scientific and technical information considered important, complete, and a lasting contribution to existing knowledge.

TECHNICAL NOTES: Information less broad in scope but nevertheless of importance as a contribution to existing knowledge.

TECHNICAL MEMORANDUMS: Information receiving limited distribution because of preliminary data, security classification, or other reasons.

CONTRACTOR REPORTS: Scientific and technical information generated under a NASA contract or grant and considered an important contribution to existing knowledge.

TECHNICAL TRANSLATIONS: Information published in a foreign language considered to merit NASA distribution in English.

SPECIAL PUBLICATIONS: Information derived from or of value to NASA activities. Publications include conference proceedings, monographs, data compilations, handbooks, sourcebooks, and special bibliographies.

TECHNOLOGY UTILIZATION PUBLICATIONS: Information on technology used by NASA that may be of particular interest in commercial and other non-aerospace applications. Publications include Tech Briefs, Technology Utilization Reports and Notes, and Technology Surveys.

*Details on the availability of these publications may be obtained from:*

SCIENTIFIC AND TECHNICAL INFORMATION DIVISION

NATIONAL AERONAUTICS AND SPACE ADMINISTRATION

Washington, D.C. 20546